Connecting between inflation and dark matter in models with gauged Z_3 symmetry

Soo-Min Choi,[a,c] **Jinsu Kim,**[b] **Hyun Min Lee**[a,c] **and Bin Zhu**[a,d]

[a]*Department of Physics, Chung-Ang University,*
Seoul 06974, Korea

[b]*Institute for Theoretical Physics, Georg-August University Göttingen,*
Friedrich-Hund-Platz 1, Göttingen D-37077, Germany

[c]*CERN, Theory department,*
1211 Geneva 23, Switzerland

[d]*School of Physics, Yantai University,*
Yantai 264005, China

E-mail: soominchoi90@gmail.com,
jinsu.kim@theorie.physik.uni-goettingen.de, hminlee@cau.ac.kr,
zhubin@mail.nankai.edu.cn

ABSTRACT: We investigate the possibility of unifying the inflation and dark matter physics in the minimal model for a complex scalar dark matter with gauged Z_3 symmetry. The dark local U(1) symmetry is broken spontaneously into the Z_3 symmetry by the dark Higgs mechanism. As compared to dark matter models with Z_2 parity, the dark matter cubic self-interaction restricts the inflation with non-minimal couplings to take place beyond the pure dark matter direction and plays an important role in the loop corrections for the inflationary predictions as well as determining the correct dark matter relic density. Considering either of $2 \to 2$, $3 \to 2$ or forbidden channels to be a dominant production mechanism for dark matter, we show the viable parameter space of the model that is consistent with the theoretical and phenomenological constraints combined from inflation and dark matter.

https://doi.org/10.1007/JHEP06(2020)135

Contents

1 Introduction

There have been a lot of progresses in measuring the cosmological parameters of the universe with unprecedented precision, for instance, from the Cosmic Microwave Background (CMB) anisotropies. Thus, two pillars in the modern cosmology, inflation [1] and dark matter [2], have reinforced the motivations and efforts for searching for physics beyond the Standard Model (SM). Inspired by the SM Higgs inflation [3], there have been recent attempts to integrate inflation in connection with low energy particle physics. Moreover, given that the nature of dark matter remains a mystery, the unification of inflation and dark matter provides an economical way of solving the problems in cosmology and particle physics at the same time [4–12]. The merit of this kind consideration is that additional fields introduced

for the consistency may also solve the problems in the SM, such as the vacuum instability of the SM Higgs potential.

Various candidates for dark matter are based on the Z_2 symmetry for guaranteeing the stability of dark matter and their production mechanism rely on the freeze-out processes in the so-called Weakly Interacting Massive Particles (WIMPs) paradigm. Inclusion of discrete symmetries beyond the Z_2 symmetry leads to interesting and new avenues for dark matter physics, such as $2 \to 2$ and $3 \to 2$ semi-annihilation processes for the freeze-out. In particular, in the latter case, the freeze-out process would require dark matter to have large self-interactions but small couplings to the SM. This possibility, so-called Strongly Interacting Massive Particles (SIMPs) paradigm [13–16] has been realized in a simple extension with gauged Z_3 symmetry [17, 18], where there are a lot of interesting signatures at intensity beam experiments and astrophysical observations of galaxy rotation curves and cluster collisions.

As inflation and dark matter physics involve largely different scales, it is important to include quantum corrections to match them by using the renormalization group (RG) equations. In particular, it is notable that inflationary observables such as the spectral index n_s and tensor-to-scalar ratio r may be significantly affected by quantum effects; for instance, the predicted value for the inflation with non-minimal coupling changes the tensor-to-scalar ratio from $r \approx 0.003$ to a somewhat larger value by quantum effects [12]. In the original Higgs inflation, the tree-level unitarity is violated due to a large non-minimal coupling at the scale much lower than the Planck scale [19–22], so there is a need of introducing new physics or degrees of freedom to solve the unitarity problem [23–27]. However, taking into account the running Higgs quartic coupling in Higgs inflation, we can tolerate a smaller value of the non-minimal coupling, as compared to the case without quantum effects, so the unitarity scale could be delayed to a higher scale at the expense of a fine-tuning in realizing the inflation near the inflection point of the potential [12].

In this article, we study the dynamics of inflation and dark matter in the unified framework beyond the Z_2 symmetry, in particular, by adopting models with gauged Z_3 symmetry. Dark matter phenomenology in the same models has been investigated for the thermal freeze-out with WIMP [28, 29] and SIMP dark matter [17, 18]. A generalization of the similar discussion was made for models with Z_5 discrete symmetry [30]. The focus of our work is to fill a gap between dark matter and inflation scales and make a consistent description of the early universe in a single framework beyond the Z_2 symmetry. The model with Z_3 symmetry consists of two complex scalar fields, one SM-singlet dark Higgs ϕ and one SM-singlet scalar dark matter χ, beyond the SM. The SM-singlet dark Higgs ϕ is responsible for the spontaneous symmetry breaking of a dark $U(1)_X$ into Z_3 symmetry, which ensures the stability of dark matter.

We cover three distinct regimes of dark matter production with WIMP, SIMP, and forbidden dark matter. We connect each of the cases to the inflationary regime for the first time. To do so, it is crucial to include nonzero non-minimal couplings to gravity for all the scalar fields, which are generated otherwise at the quantum level in curved spacetime. We regard a slow-roll inflation as taking place along the flat direction in the system of two real scalar fields, one of which is frozen in the minimum of the potential during inflation. Thus,

the dynamics of inflation is reduced down effectively to the case of a single-field inflation. The effective inflaton can be either the dark Higgs or a mixture of the dark Higgs and scalar dark matter [31]. We note, however, that it is impossible for the scalar dark matter χ solely to play the role of inflaton; namely the pure χ field direction is not at the minimum of the potential. This is one of the distinctive features of the Z_3 models in comparison to the Z_2 models where scalar dark matter can be the only inflaton. We connect between dark matter and inflation scales by employing the RG-improved effective action and look for the consistent parameter space with the correlations between the following relevant observables: the relic density on one side, and perturbativity, unitarity and stability on the other side.

The paper is organized as follows. We begin with a description of our setup in section 2, with a complete model Lagrangian and the particle content. In section 3, we first discuss the details on the inflationary dynamics at the classical level and include the RG effects in the later part. In this section, inflationary observables such as the spectral index and tensor-to-scalar ratio are computed. We continue to discuss the general Boltzmann equation for dark matter and focus on three distinct limits of production mechanism of dark matter in section 4, and then impose the consistency conditions for connecting between inflation and dark matter scales, such as stability, perturbativity and unitarity as well as various constraints from low-energy experiments. Finally, conclusions are drawn in section 5. There are two appendices providing the formulas for the RG equations and dark matter annihilation and scattering cross sections.

2 The model

We consider an extension of the SM with a local dark $U(1)_X$, including one complex scalar ϕ for dark Higgs mechanism and one complex scalar χ for dark matter. Then, the Lagrangian of our model [18] is given by

$$\mathcal{L} = \mathcal{L}_{NM} + \mathcal{L}_{SM} + \mathcal{L}_X + \mathcal{L}_{portal}, \tag{2.1}$$

where $\mathcal{L}_{SM}$ is the SM Lagrangian,

$$\mathcal{L}_{NM} = \frac{M_P^2}{2}\left(1 + 2\xi_\chi\frac{|\chi|^2}{M_P^2} + 2\xi_\phi\frac{|\phi|^2}{M_P^2} + 2\xi_H\frac{|H|^2}{M_P^2}\right)\mathcal{R}, \tag{2.2}$$

describes the non-minimal couplings of the scalar fields to gravity, and

$$\mathcal{L}_X = -\frac{1}{4}V_{\mu\nu}V^{\mu\nu} + (D_\mu\chi)^\dagger(D^\mu\chi) + (D_\mu\phi)^\dagger(D^\mu\phi) + m_\phi^2|\phi|^2 - m_\chi^2|\chi|^2$$
$$- \lambda_\phi|\phi|^4 - \lambda_\chi|\chi|^4 - \lambda_{\phi\chi}|\phi|^2|\chi|^2 - \zeta\phi^\dagger\chi^3 - \zeta\phi(\chi^\dagger)^3, \tag{2.3}$$

$$\mathcal{L}_{portal} = -\lambda_{\phi H}|\phi|^2|H|^2 - \lambda_{\chi H}|\chi|^2|H|^2 - \frac{1}{2}\sin\xi\, B_{\mu\nu}V^{\mu\nu}. \tag{2.4}$$

The action is then given by $S = \int d^4x\sqrt{-g}\mathcal{L}$. The SM Higgs doublet is denoted by H, ϕ is an SM-singlet complex field dubbed the dark Higgs, and χ is another SM-singlet complex field. The covariant derivatives are given by

$$D_\mu\phi = (\partial_\mu - iq_\phi g_X V_\mu)\phi, \qquad D_\mu\chi = (\partial_\mu - iq_\chi g_X V_\mu)\chi, \tag{2.5}$$

with g_X being the gauge coupling of the dark U(1)$_X$ group. Here $V_{\mu\nu} = \partial_\mu V_\nu - \partial_\nu V_\mu$ is the field strength tensor for U(1)$_X$, and $\sin\xi$ is the gauge kinetic mixing between the SM hypercharge and U(1)$_X$. Note that $\zeta = \sqrt{2}\kappa/3!$ as compared to ref. [18].

We consider the complex scalar χ as a dark matter candidate, having a charge $q_\chi = 1$ under the dark U(1)$_X$ symmetry. Another field ϕ, which has a charge $q_\phi = 3$, takes a vacuum expectation value (VEV) by $\langle\phi\rangle = v_\phi/\sqrt{2}$, and thus, being responsible for the spontaneous symmetry breaking of U(1)$_X$ into Z_3. Therefore the remaining discrete Z_3 symmetry guarantees the dark matter stability. Moreover, the U(1)$_X$ gauge boson receives mass, $m_{Z'} = 3g_X v_\phi$, and the dark Higgs mass becomes, $m_{h'} = \sqrt{2\lambda_\phi}\, v_\phi$, in the limit of a vanishing $\lambda_{\phi H}$; see ref. [18] for details. We note that when the dark Higgs ϕ carries $q_\phi = +5$, the U(1)$_X$ gauge symmetry is broken down to Z_5, for which single or multi-component dark matter scenarios were also discussed [30].

2.1 The inflation regime

For our discussion on the inflation dynamics in the next section, we further expand the Lagrangian (2.1) by choosing the unitary gauges for the SM Higgs doublet and the dark Higgs field as $H^T = (0, h)/\sqrt{2}$ and $\phi = \varphi/\sqrt{2}$, and taking the scalar dark matter to be $\chi = \psi e^{i\gamma}/\sqrt{2}$. The scalar part of the Lagrangian (2.1) then becomes

$$\mathcal{L}_{\rm NM} = \frac{M_{\rm P}^2}{2}\left(1 + \xi_\chi \frac{\psi^2}{M_{\rm P}^2} + \xi_\phi \frac{\varphi^2}{M_{\rm P}^2} + \xi_H \frac{h^2}{M_{\rm P}^2}\right)\mathcal{R}\,, \tag{2.6}$$

$$\mathcal{L}_{\rm SM} \supset \frac{1}{2}(\partial_\mu h)^2 + \frac{1}{2}m_H^2 h^2 - \frac{1}{4}\lambda_H h^4\,, \tag{2.7}$$

$$\mathcal{L}_X = \frac{1}{2}(\partial_\mu\varphi)^2 + \frac{1}{2}(\partial_\mu\psi)^2 + \frac{1}{2}\psi^2(\partial_\mu\gamma)^2 + \frac{1}{2}m_\phi^2\varphi^2 - \frac{1}{2}m_\chi^2\psi^2$$
$$- \frac{1}{4}\lambda_\phi\varphi^4 - \frac{1}{4}\lambda_\chi\psi^4 - \frac{1}{4}\lambda_{\phi\chi}\varphi^2\psi^2 - \frac{1}{2}\zeta\varphi\psi^3\cos(3\gamma)\,, \tag{2.8}$$

$$\mathcal{L}_{\rm portal} = -\frac{1}{4}\lambda_{\phi H}\varphi^2 h^2 - \frac{1}{4}\lambda_{\chi H}\psi^2 h^2\,. \tag{2.9}$$

We assume that the SM Higgs field rolls down rapidly to its VEV during inflation, due to the initial condition or the effective mass larger than the Hubble scale, so we set $h = 0$. The relevant Lagrangian for inflation is then given by

$$\mathcal{L}_{\rm inf} = \frac{M_{\rm P}^2}{2}\left(1 + \xi_\phi \frac{\varphi^2}{M_{\rm P}^2} + \xi_\chi \frac{\psi^2}{M_{\rm P}^2}\right)\mathcal{R} + \frac{1}{2}(\partial_\mu\varphi)^2 + \frac{1}{2}(\partial_\mu\psi)^2 + \frac{1}{2}\psi^2(\partial_\mu\gamma)^2 - V(\varphi,\psi,\gamma)\,, \tag{2.10}$$

where the scalar potential reads

$$V(\varphi,\psi,\gamma) = -\frac{1}{2}m_\phi^2\varphi^2 + \frac{1}{2}m_\chi^2\psi^2 + \frac{1}{4}\lambda_\phi\varphi^4 + \frac{1}{4}\lambda_\chi\psi^4 + \frac{1}{4}\lambda_{\phi\chi}\varphi^2\psi^2 + \frac{1}{2}\zeta\varphi\psi^3\cos(3\gamma)\,. \tag{2.11}$$

For the inflationary period, we are interested in the large-field limit, $\xi_\phi\varphi^2/M_{\rm P}^2 + \xi_\chi\psi^2/M_{\rm P}^2 \gg 1$, so we can drop the scalar mass terms. After minimizing the scalar potential for the phase γ of scalar dark matter for $\varphi \neq 0, \psi \neq 0$, we obtain the Jordan-frame potential as

$$V_{\rm inf}(\varphi,\psi) = \frac{1}{4}\lambda_\phi\varphi^4 + \frac{1}{4}\lambda_\chi\psi^4 + \frac{1}{4}\lambda_{\phi\chi}\varphi^2\psi^2 - \frac{1}{2}\zeta\varphi\psi^3\,. \tag{2.12}$$

We will present the detailed discussion on the decoupling of the phase γ or the scalar dark matter χ for the general inflationary trajectories in section 3.3.

As a consequence, the Jordan-frame action in eq. (2.1) relevant for inflation becomes

$$S_{\text{inf}} = \int d^4x \, \sqrt{-g} \left\{ \frac{M_{\text{P}}^2}{2} \left(1 + \xi_\phi \frac{\varphi^2}{M_{\text{P}}^2} + \xi_\chi \frac{\psi^2}{M_{\text{P}}^2} \right) \mathcal{R} + \frac{1}{2}(\partial_\mu \varphi)^2 + \frac{1}{2}(\partial_\mu \psi)^2 \right.$$
$$\left. - \frac{1}{4}\lambda_\phi \varphi^4 - \frac{1}{4}\lambda_\chi \psi^4 - \frac{1}{4}\lambda_{\phi\chi}\varphi^2\psi^2 + \frac{1}{2}\zeta\varphi\psi^3 \right\}. \tag{2.13}$$

Then, the effective theory for inflation is a system of two real scalar fields with quartic couplings and non-minimal couplings, which has been extensively studied in ref. [31]. For the analysis of inflationary observables, it is convenient to work in the Einstein frame where the gravity action takes the standard form of Einstein-Hilbert action. Making a Weyl transformation to the Einstein frame by

$$\tilde{g}_{\mu\nu} = \Omega^2 g_{\mu\nu} \tag{2.14}$$

with

$$\Omega^2 = 1 + \xi_\phi \frac{\varphi^2}{M_{\text{P}}^2} + \xi_\chi \frac{\psi^2}{M_{\text{P}}^2}, \tag{2.15}$$

we obtain the following Einstein-frame action:

$$S_{\text{inf}} = \int d^4x \, \sqrt{-\tilde{g}} \left\{ \frac{M_{\text{P}}^2}{2} \tilde{\mathcal{R}} + \frac{3}{4} M_{\text{P}}^2 \tilde{g}^{\mu\nu} \partial_\mu \ln \Omega^2 \partial_\nu \ln \Omega^2 \right.$$
$$\left. + \frac{1}{2\Omega^2} \tilde{g}^{\mu\nu} \partial_\mu \varphi \partial_\nu \varphi + \frac{1}{2\Omega^2} \tilde{g}^{\mu\nu} \partial_\mu \psi \partial_\nu \psi - U \right\}, \tag{2.16}$$

where the tilde indicates the quantities associated with the Einstein-frame metric $\tilde{g}_{\mu\nu}$, and the scalar potential in the Einstein frame is given by $U = V_{\text{inf}}/\Omega^4$.

We will discuss the details of the inflation regime in section 3. The dimensionless parameters in the inflation regime are matched to low energy parameters for dark matter in the same section, thanks to the RG equations given in appendix A.

2.2 The dark matter regime

For the discussion of dark matter annihilations, expanding the SM and dark Higgs fields by $H^T = (0, v_{\text{ew}} + h)/\sqrt{2}$ and $\phi = (v_\phi + h')/\sqrt{2}$, and diagonalizing the scalar and neutral gauge boson mass matrices, we can obtain various interaction terms for scalar dark matter χ [17, 18]. We denote the CP-even scalars and dark gauge-like bosons by $h_{1,2}$ and Z', respectively.

The interaction Lagrangian for dark matter with Higgs and Z' portals at low energy is given [17] by

$$\mathcal{L}_{\text{int}} = -(\lambda_{\phi\chi} v_\phi \cos\theta - \lambda_{\chi H} v_{\text{ew}} \sin\theta) h_1 |\chi|^2 - (\lambda_{\phi\chi} v_\phi \sin\theta + \lambda_{\chi H} v_{\text{ew}} \cos\theta) h_2 |\chi|^2$$
$$- (\lambda_\phi v_\phi \cos^3\theta - \lambda_H v_{\text{ew}} \sin^3\theta) h_1^3 - 3 \sin\theta \cos\theta (\lambda_\phi v_\phi \cos\theta + \lambda_H v_{\text{ew}} \sin\theta) h_1^2 h_2$$
$$- 3 \sin\theta \cos\theta (\lambda_\phi v_\phi \sin\theta + \lambda_H v_{\text{ew}} \cos\theta) h_1 h_2^2 - (\lambda_\phi v_\phi \sin^3\theta + \lambda_H v_{\text{ew}} \cos^3\theta) h_1^3$$
$$- \frac{1}{\sqrt{2}} \zeta \left(\cos\theta \, h_1 + \sin\theta \, h_2\right) \chi^3 + \text{h.c.} - \lambda_\chi |\chi|^4 + \cdots$$
$$+ g_X Z'_\mu J_D^\mu + e \, \varepsilon Z'_\mu J_{\text{EM}}^\mu, \tag{2.17}$$

where θ is the Higgs mixing angle, and J_D^μ, J_{EM}^μ are dark and electromagnetic currents, respectively, given by $J_D^\mu = -iq_\chi(\chi\partial^\mu\chi^* - \chi^*\partial^\mu\chi)$ and $J_{EM}^\mu = Q_f\bar{f}\gamma^\mu f - iQ_W(W^\nu\partial^\mu W_\nu^\dagger - W_\mu^\dagger\partial^\mu W_\nu)$, and $\varepsilon \simeq \cos\theta_W\xi$ for $\xi \ll 1$. Here, the ellipsis in the fourth line corresponds to the quartic couplings for CP-even scalars, which are reduced to $-\frac{1}{4}\lambda_\phi h_1^4 - \frac{1}{4}\lambda_H h_2^4$ in the limit of a vanishing Higgs mixing angle. Henceforth, we denote $h_1 \approx h'$ for a small Higgs mixing angle.

As a consequence, dark matter can annihilate into a pair of the SM particles through Higgs and Z' portal couplings for nonzero θ and ε. Moreover, dark matter can also annihilate into the dark sector, such as $\chi\chi \to \chi^*A'$, $\chi\chi^* \to AA$ with $A = h', Z'$. When the self-interaction of dark matter is sizable, dark matter can also annihilate by $3 \to 2$ processes, such as $\chi\chi\chi \to \chi\chi^*$, $\chi\chi\chi^* \to \chi^*\chi^*$, and $\chi\chi\chi^* \to \chi A$ with $A = h', Z'$. The details on the Boltzmann equation for determining the relic density, $n_{DM} = n_\chi + n_{\chi*}$, are presented in appendix B. For the later discussion, we assume that dark Higgs h' and dark photon Z' are in thermal equilibrium with the SM thermal bath, so we can take $n_{h'} = n_{h'}^{eq}$ and $n_{Z'} = n_{Z'}^{eq}$. Using the expressions for all the dark matter annihilation cross sections summarized in appendix B, we will determine the dark matter relic density in section 4.

3 Inflationary dynamics

In this section, we discuss the details of the dynamics of inflation and constraints in our model. We also discuss the justification of decoupling the extra scalar degree(s) of freedom for the effective theory of inflation.

3.1 Inflation in large-field limit

Closely following the discussion in ref. [31] and making the field redefinitions with

$$\sigma \equiv \sqrt{\frac{3}{2}}M_P \ln\Omega^2, \quad \tau \equiv \frac{\varphi}{\psi}, \tag{3.1}$$

we rewrite the scalar kinetic terms and potential in the Einstein frame, respectively, as

$$\begin{aligned}
\mathcal{L}_{kin} &= \frac{1}{2}\frac{M_P^2(\xi_\chi^2 + \xi_\phi^2\tau^2)}{(\xi_\chi + \xi_\phi\tau^2)^3}\left(1 - e^{-\sqrt{\frac{2}{3}}\frac{\sigma}{M_P}}\right)(\tilde{\partial}\tau)^2 \\
&\quad + \frac{1}{2}\left(\frac{e^{\sqrt{\frac{2}{3}}\frac{\sigma}{M_P}}(1 + 6\xi_\chi + (1 + 6\xi_\phi)\tau^2) - 6(\xi_\chi + \xi_\phi\tau^2)}{6(\xi_\chi + \xi_\phi\tau^2)(e^{\sqrt{\frac{2}{3}}\frac{\sigma}{M_P}} - 1)}\right)(\tilde{\partial}\sigma)^2 \\
&\quad + \frac{M_P(\xi_\chi - \xi_\phi)\tau}{\sqrt{6}(\xi_\chi + \xi_\phi\tau^2)^2}(\tilde{\partial}\sigma)(\tilde{\partial}\tau),
\end{aligned} \tag{3.2}$$

and

$$U = U_0(\tau)\left(1 - e^{-\sqrt{\frac{2}{3}}\frac{\sigma}{M_P}}\right)^2, \tag{3.3}$$

with

$$U_0(\tau) \equiv \frac{M_P^4(\lambda_\chi - 2\zeta\tau + \lambda_{\phi\chi}\tau^2 + \lambda_\phi\tau^4)}{4(\xi_\chi + \xi_\phi\tau^2)^2}. \tag{3.4}$$

In the large-field limit for inflation, the kinetic terms become approximated to

$$\mathcal{L}_{\rm kin} \simeq \frac{1}{2}(\tilde{\partial}\sigma)^2 + \frac{1}{2}\frac{M_{\rm P}^2(\xi_\chi^2 + \xi_\phi^2\tau^2)}{(\xi_\chi + \xi_\phi\tau^2)^3}(\tilde{\partial}\tau)^2 + \frac{M_{\rm P}(\xi_\chi - \xi_\phi)\tau}{\sqrt{6}(\xi_\chi + \xi_\phi\tau^2)^2}(\tilde{\partial}\sigma)(\tilde{\partial}\tau)$$

$$\simeq \frac{1}{2}(\tilde{\partial}\sigma)^2 + \frac{1}{2}(\tilde{\partial}\tau_c)^2 + (\tilde{\partial}\sigma)(\tilde{\partial}\tau_c)\frac{(\xi_\chi - \xi_\phi)\tau}{\sqrt{6}\sqrt{\xi_\chi^2 + \xi_\phi^2\tau^2}\sqrt{\xi_\chi + \xi_\phi\tau^2}}\,, \tag{3.5}$$

where, in the second line, we used the canonical scalar field τ_c with

$$\left(\frac{d\tau_c}{d\tau}\right)^2 = \frac{M_{\rm P}^2(\xi_\chi^2 + \xi_\phi^2\tau^2)}{(\xi_\chi + \xi_\phi\tau^2)^3}\,. \tag{3.6}$$

Here, we find that the kinetic mixing term is suppressed by $1/\sqrt{\xi_\chi + \xi_\phi\tau^2}$ with large non-minimal couplings. As a result, it is sufficient to consider the effective action in the later discussion on inflation in the following form,

$$S_{\rm inf} = \int d^4x\,\sqrt{-\tilde{g}}\left\{\frac{M_{\rm P}^2}{2}\tilde{\mathcal{R}} + \frac{1}{2}(\tilde{\partial}\sigma)^2 + \frac{1}{2}(\tilde{\partial}\tau_c)^2 - U\right\}. \tag{3.7}$$

We note that there is no symmetry exchanging between φ and ψ, leading to $\tau \to 1/\tau$, for a nonzero value ζ and unequal values of non-minimal couplings. Therefore, we will show in the next subsection that the ratio of the fields, τ, is stabilized at a nonzero value by the potential $U_0(\tau)$ in eq. (3.4). We will take the non-minimal couplings to equal values in some benchmark models for dark matter in the later discussion, but there is no symmetry associated with $\tau \to 1/\tau$ due to the cubic coupling for dark matter, ζ. In the limit of a vanishing ζ, the above effective Lagrangian coincides with the one with self-quartic and mixing quartic couplings only, known in the literature [31].

3.2 Inflationary minima

In order to guarantee the stability of a single-field inflation with the σ field, we impose the following conditions on the minimum of the potential with respect to $\tau = \tau_m$,

$$U\bigg|_{\tau=\tau_m} \geq 0\,, \quad \frac{\partial U}{\partial \tau_c}\bigg|_{\tau=\tau_m} = 0\,, \quad \frac{\partial^2 U}{\partial \tau_c^2}\bigg|_{\tau=\tau_m} \geq 0\,. \tag{3.8}$$

Once τ_m is fixed by the minimization of the potential, the vacuum energy during inflation is given accordingly by $U_0(\tau_m)$ with eq. (3.4). For the forthcoming discussion on the inflationary minima, we note that the first and second derivatives of the inflation potential with respect to τ_c are given, respectively, by

$$\frac{\partial U}{\partial \tau_c} \approx \frac{M_{\rm P}^3}{2(\xi_\chi + \xi_\phi\tau^2)^{3/2}\sqrt{\xi_\chi^2 + \xi_\phi^2\tau^2}}\bigg[-\zeta\xi_\chi + (\lambda_{\phi\chi}\xi_\chi - 2\lambda_\chi\xi_\phi)\tau$$

$$+ 3\zeta\xi_\phi\tau^2 + (2\lambda_\phi\xi_\chi - \lambda_{\phi\chi}\xi_\phi)\tau^3\bigg] \tag{3.9}$$

and

$$\frac{\partial^2 U}{\partial \tau_c^2} \approx \frac{M_{\mathrm{P}}^2}{2(\xi_\chi + \xi_\phi \tau^2)(\xi_\chi^2 + \xi_\phi^2 \tau^2)^2} \bigg\{ 2\lambda_\chi \xi_\phi \left(3\xi_\phi^3 \tau^4 + 2\xi_\phi \xi_\chi^2 \tau^2 - \xi_\chi^3 \right)$$
$$+ \lambda_{\phi\chi} \left(\xi_\phi^4 \tau^6 - 5\xi_\phi^3 \xi_\chi \tau^4 - 5\xi_\phi \xi_\chi^3 \tau^2 + \xi_\chi^4 \right)$$
$$+ \tau \left[2\lambda_\phi \xi_\chi \tau \left(3\xi_\chi^3 + 2\xi_\phi^2 \xi_\chi \tau^2 - \xi_\phi^3 \tau^4 \right) \right.$$
$$\left. + \zeta \xi_\phi \left(9\xi_\chi^3 + \xi_\phi \xi_\chi^2 + \xi_\phi \xi_\chi (7\xi_\phi - 3\xi_\chi)\tau^2 - 6\xi_\phi^3 \tau^4 \right) \right] \bigg\} . \qquad (3.10)$$

3.2.1 Dark matter inflaton

From the first derivative of the potential in eq. (3.9), it is easy to see that $\tau = \varphi/\psi = 0$ would not be an extremum for $\zeta \xi_\chi \neq 0$, due to the linear potential term. Thus, the inflation with pure dark matter (ψ) is not possible for $\zeta \neq 0$. (We note that $\xi_\chi = 0$ is not a fixed point under RG; see appendix A.) This shows a clear distinction from the dark matter scenarios with Z_2 symmetry where the inflation with pure dark matter becomes a stable minimum. Since the case with Z_2 symmetry has been extensively discussed in the literature, we focus on the case with $\zeta \neq 0$, so we do not pursue any longer the inflation scenario with pure dark matter in the later discussion.

3.2.2 Dark Higgs inflaton

We find that $\tau = \varphi/\psi = \infty$, corresponding to the inflation with pure dark Higgs, is always an extremum of the potential, independent of ζ. From the second derivative of the potential (3.10), we find that

$$\frac{\partial^2 U}{\partial \tau_c^2} = \frac{M_{\mathrm{P}}^2}{2\xi_\phi^2} \left(\lambda_{\phi\chi} \xi_\phi - 2\lambda_\phi \xi_\chi \right) \qquad (3.11)$$

at $\tau = \infty$. Therefore, $\tau = \infty$ is the minimum if

$$\lambda_{\phi\chi} \xi_\phi - 2\lambda_\phi \xi_\chi > 0 , \qquad (3.12)$$

or it is an inflection point if

$$\lambda_{\phi\chi} \xi_\phi - 2\lambda_\phi \xi_\chi = 0 . \qquad (3.13)$$

3.2.3 Mixed inflaton

In order to obtain the inflationary minimum with a finite τ, one needs to solve the cubic equation, the solutions to which we do not present here, due to lengthy expressions. The general solution is known, determined by the discriminant D, given by

$$\frac{D}{4} = 27\zeta^4 \xi_\phi^3 \xi_\chi + (\lambda_{\phi\chi}\xi_\phi - 2\lambda_\phi\xi_\chi)(\lambda_{\phi\chi}\xi_\chi - 2\lambda_\chi\xi_\phi)^3$$
$$+ 9\zeta^2 \left[\lambda_\chi^2 \xi_\phi^4 + \lambda_{\phi\chi}^2 \xi_\phi^2 \xi_\chi^2 - 3\lambda_\phi^2 \xi_\chi^4 + 2\lambda_\chi \xi_\phi^2 \xi_\chi (3\lambda_\phi \xi_\chi - 2\lambda_{\phi\chi}\xi_\chi) \right] . \qquad (3.14)$$

If $D > 0$, there exist three real values for τ; if $D < 0$ there exists only one real value for τ. Thus, there exists at least one minimum for a finite τ. Taking $\tau > 0$ and using the

second derivative of the potential in eq. (3.10), we can find the value for τ_m that satisfies the inflation conditions (3.8).

For a finite value of τ, the inflaton is a mixture of the dark Higgs (φ) and dark matter (ψ). Then, taking $\tau = \tau_m$ to be constant along the inflation direction, we can write down the Jordan-frame action as follows:

$$
S = \int d^4 x \sqrt{-g} \left\{ \frac{M_{\mathrm{P}}^2}{2} \left[1 + \left(\xi_\chi + \xi_\phi \tau_m^2 \right) \frac{\psi^2}{M_{\mathrm{P}}^2} \right] \mathcal{R} \right.
$$
$$
\left. + \frac{1 + \tau_m^2}{2} g^{\mu\nu} \partial_\mu \psi \partial_\nu \psi - \frac{1}{4} (\lambda_\chi - 2\zeta \tau_m + \lambda_{\phi\chi} \tau_m^2 + \lambda_\phi \tau_m^4) \psi^4 \right\} . \tag{3.15}
$$

Redefining $\Phi \equiv \sqrt{1 + \tau_m^2}\, \psi$, the above action becomes

$$
S = \int d^4 x \sqrt{-g} \left\{ \frac{M_{\mathrm{P}}^2}{2} \left(1 + \xi_\Phi \frac{\Phi^2}{M_{\mathrm{P}}^2} \right) \mathcal{R} + \frac{1}{2} g^{\mu\nu} \partial_\mu \Phi \partial_\nu \Phi - \frac{1}{4} \lambda_\Phi \Phi^4 \right\} , \tag{3.16}
$$

where

$$
\xi_\Phi \equiv \frac{\xi_\chi + \xi_\phi \tau_m^2}{1 + \tau_m^2} , \qquad \lambda_\Phi \equiv \frac{\lambda_\chi - 2\zeta \tau_m + \lambda_{\phi\chi} \tau_m^2 + \lambda_\phi \tau_m^4}{(1 + \tau_m^2)^2} . \tag{3.17}
$$

Therefore, we obtain a single-field inflation for Φ with the effective parameters ξ_Φ and λ_Φ.

Unlike the inflation along the single field direction, that is, dark Higgs inflation, the effective inflaton quartic coupling can be very small due to the cancellation with the ζ parameter in the definition of λ_Φ in eq. (3.17). Then, fixing the combination $\lambda_\Phi / \xi_\Phi^2$ by the Planck normalization, we can take a small effective non-minimal coupling ξ_Φ, as will be shown shortly. Consequently, the violation of tree-level unitarity can occur at a higher scale than the case with a large non-minimal coupling.

3.3 Decoupling of the extra degree(s) of freedom from dark matter

In the previous subsections, we chose $\Omega^2 \gg 1$ for a slow-roll inflation during which the field values of φ and ψ are almost constant: 1) dark Higgs inflaton with $\varphi \neq 0$ and $\psi = 0$; 2) mixed inflaton with $\varphi \sim \psi \neq 0$.

First, for the case with $\varphi \neq 0$ and $\psi \neq 0$, which is called the mixed inflaton, ignoring the mass terms, the part of the Lagrangian in eq. (2.10) for the phase γ during inflation is given in Einstein frame by

$$
\mathcal{L}_\gamma = \frac{1}{2\Omega^2} \psi^2 (\partial_\mu \gamma)^2 - \frac{1}{2\Omega^4} \zeta \varphi \psi^3 \cos(3\gamma). \tag{3.18}
$$

Then, for $\xi_\phi \sim \xi_\chi$ and $\varphi \sim \psi$, we get $\Omega^2 \sim 2\xi_\phi \varphi^2$. Here, we set $M_P = 1$. In this case, we simplify the above Lagrangian for the canonical field, $\gamma \sim \sqrt{2\xi_\phi}\, \tilde{\gamma}$, in the following,

$$
\mathcal{L}_{\tilde{\gamma}} \simeq \frac{1}{2} (\partial_\mu \tilde{\gamma})^2 - \frac{\zeta}{8\xi_\phi^2} \cos\left(3\sqrt{2\xi_\phi}\, \tilde{\gamma} \right). \tag{3.19}
$$

Therefore, for $\zeta > 0$, expanding the phase as $3\sqrt{2\xi_\phi}\, \tilde{\gamma} = \pi + 3\sqrt{2\xi_\phi}\, \delta\tilde{\gamma}$, we can identify the squared mass of the perturbation $\delta\tilde{\gamma}$ as $m_{\delta\tilde{\gamma}}^2 \sim \frac{9\zeta}{4\xi_\phi}$, which is much greater than the squared

Hubble parameter, $H^2 = \frac{\lambda_\Phi}{4\xi_\Phi^2}$ with $\xi_\Phi \sim \xi_\phi \gg 1$ and a sizable ζ. As a result, we can safely ignore the dynamics of the phase of the scalar dark matter during inflation.

Next, for $\varphi \neq 0$ and $\psi = 0$, the radial coordinate representation for the scalar dark matter, $\chi = \psi\, e^{i\gamma}/\sqrt{2}$, is not a valid description. In this case, instead we can take $\chi = (\psi + ib)/\sqrt{2}$ in the Cartesian representation with b being a pseudo-scalar field. Then, ignoring the mass terms, the part of the Lagrangian in eq. (2.10) for the scalar dark matter including the mixing quartic coupling is given by

$$\mathcal{L}_{\psi,b} = \frac{1}{2\Omega^2}\Big((\partial_\mu\psi)^2 + (\partial_\mu b)^2\Big) - \frac{1}{4\Omega^4}\,\lambda_{\phi\chi}(\psi^2 + b^2)\varphi^2. \tag{3.20}$$

Then, taking $\Omega^2 \simeq \xi_\phi\varphi^2$ during inflation and canonically normalizing the dark scalars by $\psi = \sqrt{\xi_\phi}\langle\varphi\rangle\,\tilde\psi$ and $b = \sqrt{\xi_\phi}\langle\varphi\rangle\,\tilde b$ with $\langle\varphi\rangle$ being an almost constant field value during inflation, we can rewrite the above Lagrangian as follows,

$$\mathcal{L}_{\tilde\psi,\tilde b} \simeq \frac{1}{2}(\partial_\mu\tilde\psi)^2 + \frac{1}{2}(\partial_\mu\tilde b)^2 - \frac{\lambda_{\phi\chi}}{4\xi_\phi}\,(\tilde\psi^2 + \tilde b^2). \tag{3.21}$$

Consequently, we obtain the squared masses for dark scalars as $m_{\tilde\psi}^2 = m_{\tilde b}^2 \sim \frac{\lambda_{\phi\chi}}{2\xi_\phi}$, which is again much larger than the squared Hubble parameter, $H^2 = \frac{\lambda_\phi}{4\xi_\phi^2}$ with $\xi_\phi \gg 1$ and a sizable $\lambda_{\phi\chi}$. As a result, we can ignore the dynamics of dark scalars in χ during inflation.

In summary, independent of the inflationary vacua, the phase of dark matter or the full complex scalar dark matter can be decoupled during inflation, thus justifying our analysis focusing on the two real scalar fields, φ and ψ, in the previous subsections. Moreover, the results show that there is no isocurvature perturbation generated along the complex scalar dark matter in any inflation minimum.

3.4 Inflationary observables

For a given potential, it is straightforward to compute inflationary observables such as the scalar power spectrum, the spectral index, and the tensor-to-scalar ratio, in terms of the inflation vacuum energy and slow-roll parameters.

In order to link inflation to dark matter physics, it is essential to include the RG effects to account for the difference in energy scales. We follow the procedures outlined in ref. [12]. Quantizing the theory in the Jordan frame and considering the RG-improved effective action, we get the leading effective action [32] as

$$\Gamma = \int d^4x\,\sqrt{-g}\,\left[\frac{M_\mathrm{P}^2}{2}\Omega^2\mathcal{R} + \frac{1}{2}g^{\mu\nu}G^2\partial_\mu\Phi\partial_\nu\Phi - V_\mathrm{eff}\right], \tag{3.22}$$

where Φ is the inflaton and

$$\Omega^2(t) = 1 + \xi_\Phi(t)G^2(t)\frac{\Phi^2(t)}{M_\mathrm{P}^2}, \tag{3.23}$$

$$V_\mathrm{eff}(t) = \frac{\lambda_\Phi(t)}{4}G^4(t)\Phi^4(t), \tag{3.24}$$

$$G(t) = \exp\left(-\int^t dt'\,\frac{\gamma_\Phi}{1+\gamma_\Phi}\right). \tag{3.25}$$

Here, $t = \ln(\mu/\mu_0)$ and μ is the renormalization scale, and we choose $\mu = \Phi$ and $\mu_0 = M_Z$. We present the RG equations determining the running couplings and anomalous dimensions in our model in appendix A. We identify the inflaton as $\Phi = \varphi$ in the dark Higgs inflation and $\Phi = \sqrt{1 + \tau_m^2}\,\psi$ in the mixed inflation.

Inflationary observables are computed in the Einstein frame. The relevant Einstein-frame potential is given by

$$U_{\rm eff} = \frac{V_{\rm eff}}{\Omega^4} = \frac{\lambda_\Phi(t)G^4(t)\Phi^4(t)}{4[1 + \xi_\Phi(t)G^2(t)\Phi^2(t)/M_{\rm P}^2]^2}\,. \tag{3.26}$$

The slow-roll parameters are then obtained from the standard definitions:

$$\epsilon = \frac{M_{\rm P}^2}{2}\left(\frac{U_{\rm eff}'}{U_{\rm eff}}\right)^2, \quad \eta = M_{\rm P}^2\frac{U_{\rm eff}''}{U_{\rm eff}}, \quad \kappa^2 = M_{\rm P}^4\frac{U_{\rm eff}'U_{\rm eff}'''}{U_{\rm eff}^2}\,, \tag{3.27}$$

where the prime represents the derivative with respect to the canonically normalized field Ψ which is related to the Jordan-frame field Φ by

$$\frac{d\Psi}{d\Phi} = \sqrt{\frac{G^2}{\Omega^2} + \frac{3M_{\rm P}^2}{2\Omega^4}\left(\frac{d\Omega^2}{d\Phi}\right)^2}\,. \tag{3.28}$$

In the classical limit of $G \to 1$, we have

$$\frac{d\Psi}{d\Phi} = \frac{\sqrt{1 + (1 + 6\xi_\Phi)\xi_\Phi\Phi^2/M_{\rm P}^2}}{1 + \xi_\Phi\Phi^2/M_{\rm P}^2}\,. \tag{3.29}$$

From the slow-roll parameters, we compute the spectral index n_s and the tensor-to-scalar ratio r at the horizon exit, as follows [33–35],

$$n_s \approx 1 - 6\epsilon + 2\eta - \frac{2}{3}(5 + 36c)\epsilon^2 + 2(-1 + 8c)\epsilon\eta + \frac{2}{3}\eta^2 + \left(\frac{2}{3} - 2c\right)\kappa^2\,, \tag{3.30}$$

$$r \approx 16\epsilon\left[1 + \left(-\frac{4}{3} + 4c\right)\epsilon + \left(\frac{2}{3} - 2c\right)\eta\right]\,, \tag{3.31}$$

where we have computed the quantities up to the second order in the slow-roll parameters and $c = \gamma + \ln 2 - 2$ with $\gamma \approx 0.5772$ being the Euler-Mascheroni constant. The number of e-foldings, N, can be also obtained from

$$N = \frac{1}{M_{\rm P}^2}\int_{\Psi_e}^{\Psi_*} d\Psi\,\frac{U_{\rm eff}}{U_{\rm eff}'}\,, \tag{3.32}$$

where Ψ_e (Ψ_*) is the canonically normalized field value at the end of inflation for $\epsilon \simeq 1$ (at the horizon exit). For typical reheating scenarios, we take $N = 60$ at the horizon exit.

Let us briefly discuss the inflation dynamics classically. From $\epsilon \simeq 1$ we find that the Jordan-frame inflaton field at the end of inflation Φ_e is given by $\Phi_e \simeq M_{\rm P}(4/3)^{1/4}/\sqrt{\xi_\Phi}$. We may then express Φ in terms of N as

$$\Phi(N) \approx \sqrt{\frac{4N}{3\xi_\Phi}}M_{\rm P}\,. \tag{3.33}$$

Then, the magnitude of the scalar power spectrum is given by

$$A_s = \frac{U_{\rm eff}}{24\pi^2 M_{\rm P}^4 \epsilon} \approx \left(\frac{N^2}{72\pi^2}\right) \frac{\lambda_\Phi}{\xi_\Phi^2} \,. \tag{3.34}$$

As mentioned earlier, the non-minimal coupling parameter ξ_Φ is chosen to satisfy the magnitude of the scalar power spectrum at the horizon exit, $A_s \approx 2.1 \times 10^{-9}$ [1].

In the large-field limit, the slow-roll parameters, ϵ and η, are expressed in terms of the number of e-foldings,

$$\epsilon \approx \frac{3}{4N^2}\,, \quad \eta \approx -\frac{1}{N}\,. \tag{3.35}$$

At the first order in the slow-roll parameters, the spectral index and the tensor-to-scalar ratio are then given by

$$n_s \approx 1 - \frac{2}{N} - \frac{9}{2N^2}\,, \quad r \approx \frac{12}{N^2}\,. \tag{3.36}$$

Therefore, we recover the well-known results for inflation with non-minimal coupling at the classical level, which are $n_s \approx 0.9654$ and $r \approx 0.003$ for $N = 60$, being consistent with Planck data [1].

We are now in a position to discuss quantum corrections for inflationary observables. To discuss effects of runnings of the parameters qualitatively, let us consider the running of the effective quartic coupling λ_Φ, ignoring the running of the non-minimal coupling for now. The slow-roll parameters, ϵ and η, in the large-field limit are then corrected [12, 24] to

$$\epsilon \approx \frac{4M_{\rm P}^4}{3\xi_\Phi^2 \Phi^4}\left[1 + \frac{\xi_\Phi \Phi^2}{4M_{\rm P}^2}\left(\frac{\beta_{\lambda_\Phi}}{\lambda_\Phi}\right)\right]^2\,, \qquad \eta \approx -\frac{4M_{\rm P}^2}{3\xi_\Phi \Phi^2}\left(1 - \frac{\beta_{\lambda_\Phi}}{2\lambda_\Phi}\right)\,, \tag{3.37}$$

where $\beta_{\lambda_\Phi} \equiv d\lambda_\Phi/dt$ is the beta function of the effective quartic coupling. Here we have ignored $d\beta_{\lambda_\Phi}/dt$ and $\beta_{\lambda_\Phi}^2$ terms.

One may relate the inflation field value Φ with the number of e-foldings N. In the presence of quantum corrections, the number of e-foldings becomes

$$N \approx \frac{3\xi_\Phi}{2M_{\rm P}^2} \int_{\Phi_e}^{\Phi_*} d\Phi\, \Phi \left[1 - \frac{\xi \Phi^2}{4M_{\rm P}^2}\left(\frac{\beta_{\lambda_\Phi}}{\lambda_\Phi}\right)\right]\,, \tag{3.38}$$

from which we obtain

$$\frac{\Phi(N)}{M_{\rm P}} \approx \sqrt{\frac{4N}{3\xi_\Phi}\left[1 + \frac{N}{6}\left(\frac{\beta_{\lambda_\Phi}}{\lambda_\Phi}\right)\right]}\,. \tag{3.39}$$

Therefore, if $\beta_{\lambda_\Phi}/\lambda_\Phi$ is positive, the inflation field value at the horizon exit becomes larger than the classical value. In terms of N, the slow-roll parameters are given by

$$\epsilon \approx \frac{3}{4N^2} + \frac{1}{4N}\left(\frac{\beta_{\lambda_\Phi}}{\lambda_\Phi}\right)\,, \quad \eta \approx -\frac{1}{N} + \left(\frac{1}{6} + \frac{1}{2N}\right)\left(\frac{\beta_{\lambda_\Phi}}{\lambda_\Phi}\right)\,. \tag{3.40}$$

The spectral index n_s and tensor-to-scalar ratio r are, up to the first order in the slow-roll parameters, given by $r \approx 16\epsilon$ and $n_s \approx 1 - 6\epsilon + 2\eta$. We thus have

$$r \approx \frac{12}{N^2} + \frac{4}{N}\left(\frac{\beta_{\lambda_\Phi}}{\lambda_\Phi}\right), \tag{3.41}$$

$$n_s \approx 1 - \frac{2}{N} - \frac{9}{2N^2} + \frac{\beta_{\lambda_\Phi}}{3\lambda_\Phi}. \tag{3.42}$$

The quantum effect may become important in two ways: (i) β_{λ_Φ} is large and/or (ii) λ_Φ is small. In particular, in the mixed inflation, increasing the ζ parameter with the other parameters being fixed, λ_Φ becomes smaller, shifting the tensor-to-scalar ratio and spectral index to a larger value, provided that β_{λ_Φ} is positive.

We remark that the reheating process can be important for making the inflationary predictions more precise, due to the fact that the total number of e-foldings depends on the equation of state of the inflaton and the reheating temperature during reheating [36]. In the later discussion on dark matter, we take dimensionless parameters of our model to be sizable for dark matter with freeze-out processes, as far as they are allowed by perturbativity and unitarity, so we expect the reheating process to be almost instantaneous and the reheating temperature to be high enough. Moreover, there are uncertainties in quantifying the preheating dynamics. However, the details of preheating or reheating dynamics do not affect the later discussion on thermal dark matter in the next section, because dark matter is quickly thermalized after reheating and the dark matter abundance is determined by the freeze-out process at a low temperature, being insensitive to reheating. Therefore, we do not elaborate on the reheating dynamics further and take the number of e-foldings to be about $N = 60$ for illustration.

3.5 Consistency conditions from inflation

We discuss the theoretical and phenomenological consistency conditions to be satisfied for inflation physics in our model. The constraints for inflation at high scales are the following:

- Dark Higgs inflation

  The stability of the inflaton potential requires

  $$\lambda_\phi > 0, \tag{3.43}$$

  $$\lambda_{\phi\chi} > 2\lambda_\phi \frac{\xi_\chi}{\xi_\phi}. \tag{3.44}$$

- Mixed inflation

  The stability of the inflaton potential at a finite value for $\tau = \tau_m$ satisfying the extremum condition (3.9) requires

  $$\lambda_\Phi = \frac{1}{(1+\tau_m^2)^2}\left(\lambda_\chi - 2\zeta\,\tau_m + \lambda_{\phi\chi}\tau_m^2 + \lambda_\phi\tau_m^4\right) > 0, \tag{3.45}$$

  $$0 = \left(\lambda_{\phi\chi} - 2\lambda_\phi\frac{\xi_\chi}{\xi_\phi}\right)\tau_m^3 - 3\zeta\tau_m^2 + \left(2\lambda_\chi - \lambda_{\phi\chi}\frac{\xi_\chi}{\xi_\phi}\right)\tau_m + \zeta\,\frac{\xi_\chi}{\xi_\phi}. \tag{3.46}$$

  We further require the second derivative of the potential (3.10) to be positive.

- Perturbativity

  We also require perturbativity on the SM and new quartic couplings,

  $$y_t < 4\pi \,, \quad g < 4\pi \,, \quad g' < 4\pi \,, \quad g_3 < 4\pi \,, \quad g_X < 4\pi \,, \quad \lambda_i < 4\pi \,, \quad \zeta < 4\pi \,, \quad (3.47)$$

  where $i = \phi, \chi, \phi\chi, \phi H$ and χH.

- CMB normalization

  The scalar power spectrum at the Planck pivot scale [1] is given by

  $$\ln(10^{10}A_s) = 3.044 \pm 0.014 \quad (68\% \text{ C.L. Planck TT,TE,EE+lowE+lensing}) \,. \quad (3.48)$$

  Then, requiring $A_s \approx 2.1 \times 10^{-9}$ at $N = 60$, we obtain the relation between the effective quartic and non-minimal couplings as follows:

  $$\frac{\lambda_\Phi}{\xi_\Phi^2} \approx 4.15 \times 10^{-10} \,. \quad (3.49)$$

  For instance, for $\lambda_\Phi \simeq 0.1 \ (10^{-7})$, the non-minimal coupling should take $\xi_\Phi \simeq 15500$ (15.5).

- Spectral index and tensor-to-scalar rato

  The latest Planck data [1] read

  $$n_s = 0.9659 \pm 0.0041 \quad (68\% \text{ C.L. Planck TT,TE,EE+lowEB+lensing}) \,, \quad (3.50)$$
  $$r < 0.11 \quad\quad\quad\quad\quad (95\% \text{ C.L. Planck TT,TE,EE+lowEB+lensing}) \,. \quad (3.51)$$

4 Connection between inflation and dark matter

In this section, we first discuss three distinct regimes of dark matter production in our model with Z_3 symmetry: WIMP, SIMP, and forbidden dark matter scenarios [17, 18]. In the following, the relic density is calculated in each case and various theoretical and experimental constraints from dark matter are listed. Then, we explore the connection between inflation and dark matter physics and impose the consistency conditions for inflation and experimental constraints on the model.

As explained in the previous section, we can take quantum corrections into account by considering the running of the couplings, which can be read from the RG equations summarized in appendix A. We choose the following input parameters,

$$m_{h'} \,, \quad m_\chi \,, \quad \theta \,, \quad \lambda_\phi \,, \quad \lambda_\chi \,, \quad \lambda_{\phi\chi} \,, \quad \lambda_{\chi H} \,, \quad \zeta \,, \quad g_X \,, \quad \xi_H \,, \quad \xi_\chi/\xi_\phi \,, \quad (4.1)$$

at the Z boson mass scale. The Z' mass is also given by $m_{Z'} = 3g_X m_{h'}/\sqrt{2\lambda_\phi}$ for the given set of parameters. Here, we ignore the RG effects of the gauge kinetic mixing $\sin\xi$ or $\varepsilon \simeq \cos\theta_W \xi$ for $\xi \ll 1$. We again stress that one of the non-minimal coupling parameters are not a free parameter. Thus we consider the ratio of the non-minimal couplings ξ_χ/ξ_ϕ together with the SM Higgs non-minimal coupling ξ_H. Since the SM Higgs does not

participate in inflationary dynamics, we always choose $\xi_H = 0$ at the Z boson mass scale. However, due to the quantum effects, ξ_H takes a non-zero value at inflationary scale.

For a chosen set of input parameters at low-energy scale, we first analyze the dark matter phenomenology by imposing various experimental and theoretical constraints on dark matter. We then run the input parameters with the RG equations up to the scale of tree-level unitarity $\mu \sim M_{\mathrm{P}}/\sqrt{\xi_\Phi}$, where ξ_Φ is the effective non-minimal coupling for the inflaton (3.17), which is $\xi_\Phi = \xi_\phi$ in dark Higgs inflation and $\xi_\Phi = (\xi_\chi + \xi_\phi \tau_m^2)/\sqrt{1 + \tau_m^2}$ in mixed inflation. We combine the stability and perturbativity constraints from inflation at high-energy scale and various theoretical and experimental constraints from dark matter at low-energy scale, as discussed in section 3 and section 4.

In the following, we present the results of our numerical analyses, dividing the parameter space into three distinct cases, depending on the dominant production mechanisms for dark matter, WIMP, SIMP, and forbidden (FBDM) scenarios. We study dark matter and inflation constraints in each case, namely, the dependencies of the relic density, the spectral index and the tensor-to-scalar ratio on the ζ parameter, which is characteristic of the Z_3 model, distinguishing it from the Z_2 models.

4.1 Consistency conditions from dark matter

The theoretical and phenomenological constraints for dark matter at low energies are the following:

- **Stability**

  We impose the stability condition given by [18]

  $$\lambda_\chi > -\frac{1}{2}\lambda_{\phi\chi}X_{\min}^2 + \frac{3}{2}|\zeta|X_{\min}\,, \tag{4.2}$$

  where

  $$X_{\min} = \begin{cases} \left(P + \sqrt{P^2 + Q^3}\right)^{1/3} + \left(P - \sqrt{P^2 + Q^3}\right)^{1/3}\,, & D > 0 \\ 2\sqrt{-Q}\cos\left(\frac{1}{3}\cos^{-1}\left(\frac{P}{\sqrt{-Q^3}}\right)\right)\,, & D < 0 \end{cases} \tag{4.3}$$

  with $D \equiv P^2 + Q^3$, $P \equiv |\zeta|/(4\lambda_\phi)$, and $Q \equiv \lambda_{\phi\chi}/(6\lambda_\phi)$. Here, writing the scalar potential with quartic couplings in the form, $V = |\chi|^4 f(X)$ where $X \equiv |\phi|/|\chi|$, we denoted $X_{\min}$ as a positive value satisfying $f'(X_{\min}) = 0$. Then, the global minimum condition, $f(X_{\min}) > 0$, gives rise to eq. (4.2) [18].

- **Unitarity**

  We impose the unitarity conditions on the squared amplitudes for dark matter self-scattering with eqs. (B.34) and (B.35):

  $$|\mathcal{M}_{\chi\chi}| < 8\pi\,, \quad |\mathcal{M}_{\chi\chi^*}| < 8\pi\,. \tag{4.4}$$

  We note that perturbativity at low scale is trivially satisfied once it is imposed at inflation scale.

- Dark matter relic density

  We impose the correct relic density for dark matter at present, given by Planck data (TT,TE,EE+lowE+lensing) [2] as

  $$\Omega_{\rm DM} h^2 = 0.1200 \pm 0.0012 \,.$$

- Higgs decays

  In the numerical analyses below, we choose the mixing angle between the SM and dark Higgs bosons such that the LHC constraints on Higgs visible and invisible decays [37] are satisfied. The current limit on the branching fraction of the Higgs invisible decay is $\mathrm{BR}(h \to \mathrm{inv}) < 0.19$ at 90% C.L.

- Direct detection bounds

  We consider Xenon10 [38], Xenon 1T [39, 40] and SENSEI-100 1yr (expected) [41] on the spin-independent cross sections for DM-nucleon and DM-electron scatterings, which are summarized in appendix B. The Xenon10 limit [38] applies for $m_\chi =$ 8.8 MeV–3 GeV, so do the Xenon 1T limits [39, 40] for $m_\chi = 6$ GeV–10 TeV. The projected limit from SENSEI-100 1yr (expected) is relevant for $m_\chi = 1$ MeV–1 GeV and $m_{Z'} = 3 m_\chi$.

- Indirect detection bounds

  The indirect bounds on dark matter annihilation channels are the following. First, the $e^+ e^-$ annihilation constraint in CMB is stringent. We thus used the result in ref. [42] to constrain the $e^+ e^-$ annihilation at $T = 0.25$ eV for the mass range between $m_\chi = 1$ MeV and 10 TeV. We also used the AMS results in refs. [43–45] to constrain the $W^+ W^-$ annihilation for the mass range between $m_\chi = 100$ GeV to 40 TeV, $\gamma\gamma$, $b\bar{b}$ annihilations for $m_\chi = 10$ GeV–10 TeV and the $e^+ e^-$ annihilation for $m_\chi = 5$ GeV–300 GeV, respectively. In our model, the di-photon annihilation channel is induced by the combination of the SM loops and the Higgs portal interaction. We also used the Fermi-LAT limit on the $W^+ W^-$ annihilation from ref. [46] for $m_\chi = m_W - 10$ TeV and the Fermi-LAT limits on the $\tau\tau$, $b\bar{b}$ annihilations from ref. [46] for $m_\chi = m_b(m_\tau) - 10$ TeV. Moreover, the Fermi-LAT limit on the $\gamma\gamma$ annihilation in ref. [47] is imposed for $m_\chi = 0.2$ GeV–1 TeV. Lastly, the HESS constraints on the $W^+ W^-, \gamma\gamma$ annihilations are taken from refs. [48, 49] for $m_\chi = 180$ GeV–67 TeV and $m_\chi = 300$ GeV–60 TeV, respectively.

- Dark matter self-scattering

  In the case of SIMP or forbidden dark matter, the self-scattering cross section can be sizable, so it can solve the small-scale problems at galaxies or can be constrained by no hint for dark matter self-interactions at galaxy clusters. Thus, we require the self-interaction cross section to be small enough to evade the bounds from Bullet Cluster [50–52] and spherical halo shapes [53]:

  $$\frac{\sigma_{\rm self}}{m_\chi} < 1 \,\mathrm{cm}^2/\mathrm{g} \,. \tag{4.5}$$

The solution to the small-scale problems at galaxies [54] might favor $\sigma_{\rm self}/m_\chi \gtrsim 0.1\,{\rm cm^2/g}$, but we do not impose the lower bound in our work by having in mind existing alternative solutions such as baryonic feedback effects.

4.2 WIMP scenarios

WIMP dark matter annihilates into the SM particles through Higgs or Z' portals, but the strong constraints for direct detection narrow down this case near the resonance regions at $m_\chi \simeq m_{h'}/2$ or $m_{Z'}/2$. The indirect detection and CMB bounds can also constrain the WIMP dark matter with sizable Higgs portal couplings for $m_\chi \lesssim 100\,{\rm GeV}$. Away from the resonance regions, we focus on the dark matter annihilations into the hidden sector, such as $\chi\chi^* \to AA$ and $\chi\chi \to \chi^* A$ with $A = h', Z'$, for which we are safe from the direct detection bounds. Moreover, for $m_\chi \gtrsim 100\,{\rm GeV}$, the indirect detection and CMB bounds are not as strong.

We take the standard $2 \to 2$ annihilation channels to be dominant for determining the dark matter relic density, resulting in the Boltzmann equation (B.1) in the following form,

$$
\begin{aligned}
\dot{n}_{\rm DM} + 3H n_{\rm DM} = &-\frac{1}{2}\langle\sigma v\rangle_{\chi\chi^*\to f\bar{f}}\Big(n_{\rm DM}^2 - (n_{\rm DM}^{\rm eq})^2\Big)\\
&-\frac{1}{2}\langle\sigma v\rangle_{\chi\chi\to\chi^* h'}\Big(n_{\rm DM}^2 - n_{\rm DM}^{\rm eq}\, n_{\rm DM}\Big) - \frac{1}{2}\langle\sigma v\rangle_{\chi\chi^*\to h'h'}\Big(n_{\rm DM}^2 - (n_{\rm DM}^{\rm eq})^2\Big)\\
&-\frac{1}{2}\langle\sigma v\rangle_{\chi\chi\to\chi^* Z'}\Big(n_{\rm DM}^2 - n_{\rm DM}^{\rm eq}\, n_{\rm DM}\Big) - \frac{1}{2}\langle\sigma v\rangle_{\chi\chi^*\to Z'Z'}\Big(n_{\rm DM}^2 - (n_{\rm DM}^{\rm eq})^2\Big)\\
\approx &-\langle\sigma v\rangle_{2\to 2}\, n_{\rm DM}^2\,,
\end{aligned}
\tag{4.6}
$$

with

$$
\begin{aligned}
(\sigma v)_{2\to 2} \equiv &\frac{1}{2}(\sigma v)_{\chi\chi^*\to f\bar{f}} + \frac{1}{2}(\sigma v)_{\chi\chi\to\chi^* h'} + \frac{1}{2}(\sigma v)_{\chi\chi^*\to h'h'}\\
&+ \frac{1}{2}(\sigma v)_{\chi\chi\to\chi^* Z'} + \frac{1}{2}(\sigma v)_{\chi\chi^*\to Z'Z'}\\
\equiv &\, a + bv^2.
\end{aligned}
\tag{4.7}
$$

Then, the relic density for WIMP dark matter is given by

$$
\Omega_{\rm DM}h^2 = 5.20 \times 10^{-10}\,{\rm GeV}^{-2}\left(\frac{10.75}{g_*}\right)^{1/2}\left(\frac{x_f}{20}\right)\left(a + \frac{3b}{x_f}\right)^{-1},
\tag{4.8}
$$

where $x_f = m_{\rm DM}/T_f$ with T_f being the freeze-out temperature.

For $m_{h'} \ll m_\chi$ and $m_{Z'} > m_\chi$, the dark matter annihilation cross section is dominated by $\chi\chi^* \to h'h'$ and $\chi\chi \to \chi^* h'$, which is approximated to

$$
\langle\sigma v\rangle_{2\to 2} \approx \frac{\zeta^2 m_{Z'}^2}{768\pi g_X^2 m_\chi^4}\left(\frac{9g_X m_\chi}{m_{Z'}} - \frac{\lambda_{\phi\chi}m_{Z'}}{g_X m_\chi}\right)^2 + \frac{\lambda_{\phi\chi}^2}{128\pi m_\chi^2}\left(1 - \frac{\lambda_{\phi\chi}m_{Z'}^2}{9g_X^2 m_\chi^2} + \frac{\lambda_\phi m_{Z'}^2}{6g_X^2 m_\chi^2}\right)^2.
\tag{4.9}
$$

Therefore, the resulting effective annihilation rate depends on the dark matter self-couplings, the cubic coupling ζ and the mixing quartic coupling $\lambda_{\phi\chi}$, as well as the resonance
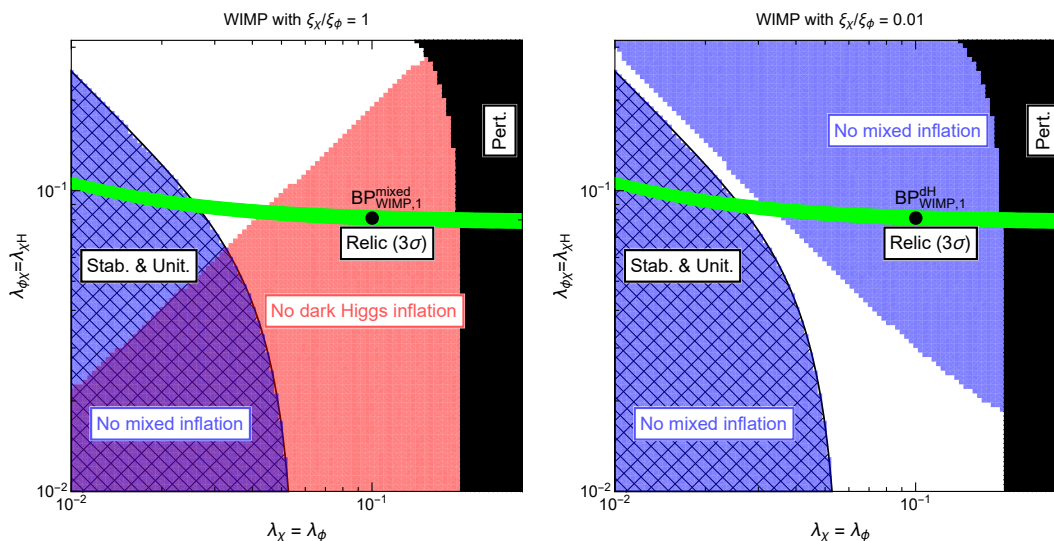
Figure 1. Parameter space for WIMP dark matter scenario with $\xi_\chi/\xi_\phi = 1$ (left) and 0.01 (right) for the quartic self-couplings with $\lambda_\chi = \lambda_\phi$ versus the quartic mixing couplings with $\lambda_{\phi\chi} = \lambda_{\chi H}$. The parameters shown here are set at low-energy scale. The rest input parameters are chosen as $\zeta = 0.05$, $g_X = 0.1$, $\sin\theta = 0.01$, $\varepsilon = 10^{-4}$, $m_{h'} = 100\,\mathrm{GeV}$ and $m_\chi = 500\,\mathrm{GeV}$. Constraints from dark matter physics and cosmic inflation are shown. The green region represents the correct dark matter relic abundance within 3σ range [2]. The hatched and black regions are disfavored due to stability, unitarity and perturbativity. The dark Higgs (mixed) inflation is not allowed in the red-colored (blue-colored) region. The black points are our benchmark points shown in table 1.

and dark matter masses. In a wide parameter space with reasonable values of the dimensionless parameters of weak strength in the model, we can make the dark matter physics consistent with the inflation regime.

In figures 1 and 2, we show various constraints coming from dark matter physics and inflation in the parameter space for the quartic self-couplings with $\lambda_\chi = \lambda_\phi$ versus the quartic mixing couplings with $\lambda_{\phi\chi} = \lambda_{\chi H}$ in the former and the quartic couplings with $\lambda_\chi = \lambda_\phi = \lambda_{\phi\chi} = \lambda_{\chi H}$ versus the dark matter cubic self-coupling ζ in the latter. Here, we chose $m_\chi = 500\,\mathrm{GeV}$ and $m_{h'} = 100\,\mathrm{GeV}$, and $m_{Z'}$ varies in the range of $60\,\mathrm{GeV} \lesssim m_{Z'} \lesssim 212\,\mathrm{GeV}$, depending on λ_ϕ in the plots. We selected four benchmark points, $\mathrm{BP^{mixed}_{WIMP,1}}$, $\mathrm{BP^{dH}_{WIMP,1}}$, $\mathrm{BP^{mixed}_{WIMP,2}}$, and $\mathrm{BP^{dH}_{WIMP,2}}$, denoted as black points in figures 1 and 2. The input parameters for those benchmark points are summarized in table 1. Imposing the normalization of the scalar power spectrum from the latest Planck, we computed inflationary observables, including the spectral index n_s and the tensor-to-scalar ratio r. The annihilation cross sections are dominated by WIMP processes in all the cases.

Our model with discrete Z_3 symmetry is distinguished from models with Z_2 through the cubic self-coupling for scalar dark matter, namely, the ζ parameter. On the left of figure 3, we show the ζ dependence of the relic density by fixing the other parameters. In comparison, on the right of figure 3, we present the relic density in the plot for the spectral index versus tensor-to-scalar ratio in order to see the correlation between dark matter and inflation constraints. We find that the spectral index and the tensor-to-scalar ratio vary, $n_s \approx 0.968$–0.974 and $r \approx 0.0028$–0.0042, depending on the ζ parameter. Thus, the spectral
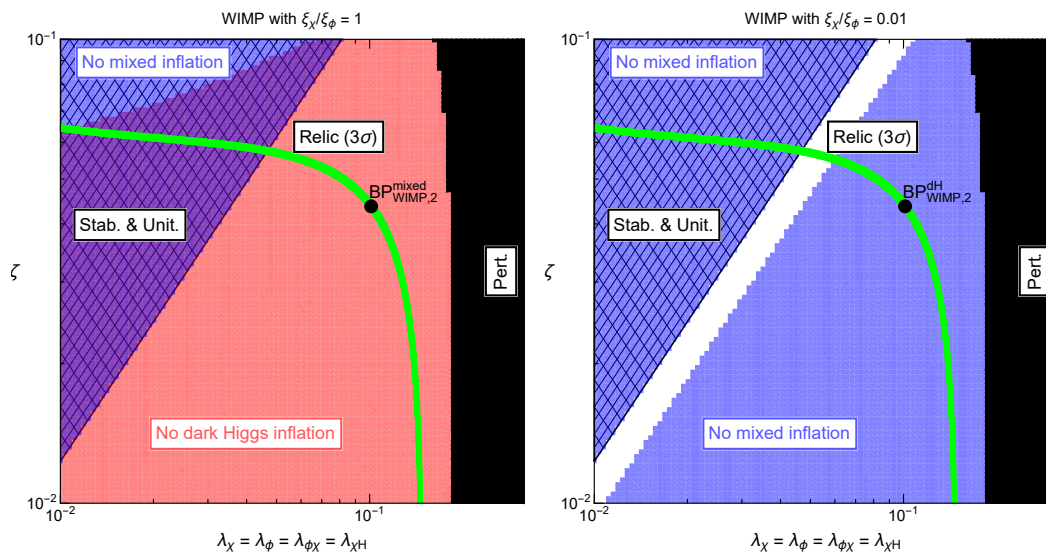
Figure 2. Parameter space for WIMP dark matter scenario with $\xi_\chi/\xi_\phi = 1$ (left) and 0.01 (right) for the quartic couplings with $\lambda_\chi = \lambda_\phi = \lambda_{\phi\chi} = \lambda_{\chi H}$ versus the dark matter cubic coupling ζ. The rest input parameters and color codes are as in figure 1, except that ζ is varying.

Benchmark Points	$\lambda_\chi = \lambda_\phi$	$\lambda_{\phi\chi} = \lambda_{\chi H}$	ζ	ξ_χ/ξ_ϕ	n_s	r
$\mathrm{BP}^{\mathrm{mixed}}_{\mathrm{WIMP},1}$	0.1	0.08	0.05	1	0.9702	0.00321
$\mathrm{BP}^{\mathrm{dH}}_{\mathrm{WIMP},1}$	0.1	0.08	0.05	0.01	0.9691	0.00296
$\mathrm{BP}^{\mathrm{mixed}}_{\mathrm{WIMP},2}$	0.1	0.1	0.04	1	0.9695	0.00306
$\mathrm{BP}^{\mathrm{dH}}_{\mathrm{WIMP},2}$	0.1	0.1	0.04	0.01	0.9691	0.00297

Table 1. Input parameters for the benchmark points, denoted as black points in figures 1 and 2. In this case, $m_{Z'}$ is also fixed to $m_{Z'} = 67\,\mathrm{GeV}$, in the upper two and lower two cases, respectively. The superscript represents the inflation type; for example, $\mathrm{BP}^{\mathrm{mixed}}_{\mathrm{WIMP},1}$ ($\mathrm{BP}^{\mathrm{dH}}_{\mathrm{WIMP},1}$) is the benchmark point where mixed (dark Higgs) inflation is allowed.

index can deviate sizably from the results of the classical non-minimal coupling inflation, but most of the parameter is still consistent with Planck within about 2σ.

4.3   SIMP scenarios

For SIMP dark matter, the dark matter abundance is determined dominantly by the $3 \to 2$ processes, which depend mostly on the dark matter self-interactions. In this case, the typical values of the dark matter mass are below GeV scale to be consistent with the correct relic density and the perturbativity bound imposed at the dark matter mass scale. But, the sizable self-couplings for dark matter would lead to the premature breakdown of perturbativity below the inflation scale. Thus, we need to rely on the enhancement of the $3 \to 2$ processes at resonances, for instance, $m_{h'} \simeq 3m_\chi$ [30, 55, 56].
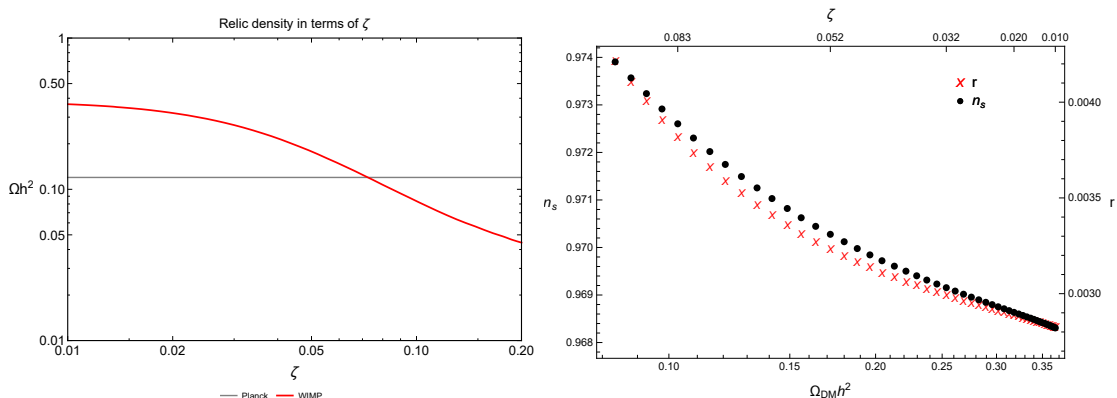
Figure 3. (Left) Relic density for WIMP dark matter as a function of ζ. (Right) Relic density in the plane of spectral index and tensor-to-scalar ratio. The parameters are chosen as follows: $\sin\theta = 0.01$, $\varepsilon = 10^{-4}$, $g_X = 0.1$, $m_{h'} = 100\,\mathrm{GeV}$, $m_\chi = 500\,\mathrm{GeV}$, $\lambda_\phi = \lambda_\chi = \lambda_{\phi\chi} = \lambda_{\chi H} = 0.1$, thus $m_{Z'} = 67\,\mathrm{GeV}$. The gray horizontal solid line on left represents the Planck data for the relic density.

We consider the case where the $3 \to 2$ annihilation processes are dominant for determining the dark matter relic density. In this case, the Boltzmann equation (B.1) becomes

$$
\begin{aligned}
\dot{n}_{\mathrm{DM}} + 3H n_{\mathrm{DM}} = &-\frac{1}{4}(\langle \sigma v^2 \rangle_{\chi\chi\chi \to \chi\chi^*} + \langle \sigma v^2 \rangle_{\chi\chi\chi^* \to \chi^*\chi^*})(n_{\mathrm{DM}}^3 - n_{\mathrm{DM}}^{\mathrm{eq}} n_{\mathrm{DM}}^2) \\
&-\frac{1}{2}\langle \sigma v^2 \rangle_{\chi\chi\chi^* \to \chi h'}\left(n_{\mathrm{DM}}^3 - (n_{\mathrm{DM}}^{\mathrm{eq}})^2 n_{\mathrm{DM}}\right) \\
&-\frac{1}{2}\langle \sigma v^2 \rangle_{\chi\chi\chi^* \to \chi Z'}\left(n_{\mathrm{DM}}^3 - (n_{\mathrm{DM}}^{\mathrm{eq}})^2 n_{\mathrm{DM}}\right) \\
\approx &-\langle \sigma v^2 \rangle_{3\to 2}\, n_{\mathrm{DM}}^3 ,
\end{aligned}
\tag{4.10}
$$

with

$$
\begin{aligned}
\langle \sigma v^2 \rangle_{3\to 2} &\equiv \frac{1}{4}(\langle \sigma v^2 \rangle_{\chi\chi\chi \to \chi\chi^*} + \langle \sigma v^2 \rangle_{\chi\chi\chi^* \to \chi^*\chi^*}) + \frac{1}{2}\langle \sigma v^2 \rangle_{\chi\chi\chi^* \to \chi h'} + \frac{1}{2}\langle \sigma v^2 \rangle_{\chi\chi\chi^* \to \chi Z'} \\
&\equiv \frac{\alpha_{\mathrm{eff}}^3}{m_\chi^5}.
\end{aligned}
\tag{4.11}
$$

Here, we note that $m_\chi < m_{h'} < 2m_\chi$ or $m_\chi < m_{Z'} < 2m_\chi$ in order for the assisted $3 \to 2$ processes with h' or Z' to be kinematically open and for the hidden sector $2 \to 2$ annihilations to be forbidden. Then, the relic density for SIMP dark matter [17, 18] is given by

$$
\Omega_{\mathrm{DM}} h^2 = 1.41 \times 10^{-8}\,\mathrm{GeV}^{-2}\left(\frac{10.75}{g_*}\right)^{3/4}\left(\frac{x_f}{20}\right)^2\left(\frac{M_{\mathrm{P}}^{1/3} m_\chi}{\alpha_{\mathrm{eff}}}\right)^{3/2}.
\tag{4.12}
$$

In the presence of the velocity-dependence or resonance poles in the $3 \to 2$ processes, special care should be taken for thermal averaging [55, 56].

For $m_{h'} \simeq 3m_\chi$, the averaged $3 \to 2$ annihilation cross section for dark matter is dominated by the resonance term in $\chi\chi\chi \to \chi\chi^*$ [55, 56], approximated to

$$
\langle \sigma v^2 \rangle \approx \frac{9\pi\zeta^2}{256 m_\chi^5}\left(1 + \frac{9\lambda_{\phi\chi}^2}{2\lambda_\phi}\right)^2 \epsilon_R^2\, x^3\, e^{-\frac{3}{2}x\,\epsilon_R}\,\theta(\epsilon_R),
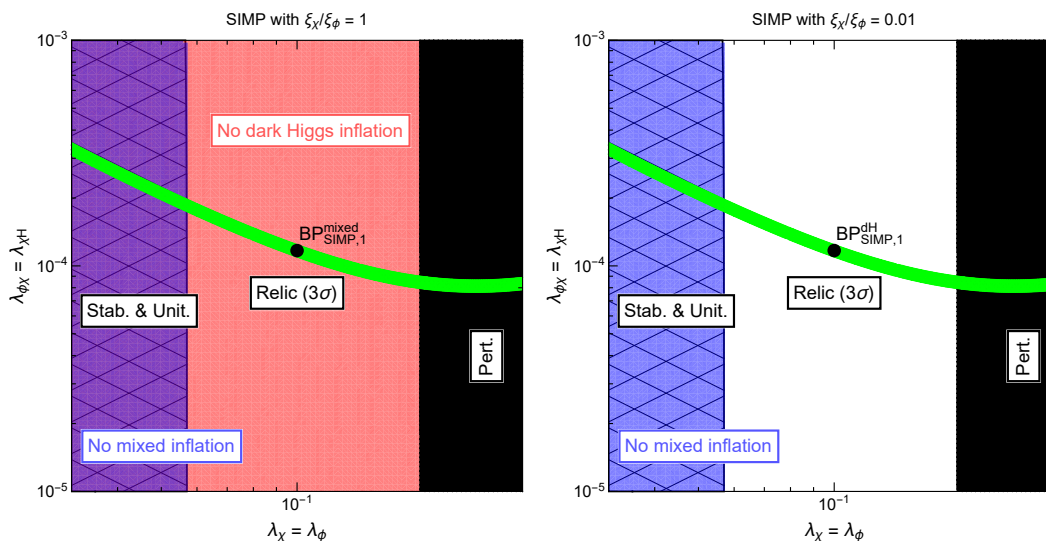\tag{4.13}
$$

Figure 4. Parameter space for SIMP dark matter scenario with $\xi_\chi/\xi_\phi = 1$ (left) and 0.01 (right), for $\lambda_\phi = \lambda_\chi$ versus $\lambda_{\phi\chi} = \lambda_{\chi H}$. The parameters shown here are set at low-energy scale. The rest input parameters are chosen as $g_X = 0.1$, $\sin\theta = 10^{-6}$, $\varepsilon = 10^{-4}$, $m_{h'} = 0.35\,\mathrm{GeV}$, $m_\chi = 0.1\,\mathrm{GeV}$ and $\zeta = 0.05$. The hatched and black regions are disfavored by stability, unitarity and perturbativity. The dark Higgs (mixed) inflation is not allowed in the red-colored (blue-colored) region. The green solid lines represent the correct dark matter relic abundance within 3σ range [2]. The black points are our benchmark points shown in table 2.

where $x = m_\chi/T$ and

$$\epsilon_R \equiv \frac{m_{h'}^2 - 9m_\chi^2}{9m_\chi^2}\,. \tag{4.14}$$

Here, we assumed the narrow width approximation with $\Gamma_{h'}/m_{h'} \ll 1, \epsilon_R$, where the width of the dark Higgs is given by $\Gamma_{h'} = \frac{\lambda_{\phi\chi}^2 v_\phi^2}{16\pi m_{h'}}\sqrt{1 - \frac{4m_\chi^2}{m_{h'}^2}}$. Then, we used the thermal average of $(\sigma v^2) = \frac{b_R\,\gamma_R}{(\epsilon_R - u^2)^2 + \gamma_R^2}$ with $\gamma_R = m_{h'}\Gamma_{h'}/(9m_\chi^2)$, $u = \frac{1}{3}(v_1^2 + v_2^2 + v_3^2)$ and b_R being a velocity-independent coefficient: $\langle\sigma v^2\rangle = \frac{27}{16}\pi\epsilon_R^2 x^3\,e^{-\frac{3}{2}x\,\epsilon_R}\,\theta(\epsilon_R)$ from ref. [55]. Therefore, the resulting effective annihilation rate depends significantly on the dark matter cubic coupling ζ as well as the resonance and dark matter masses.

In figures 4 and 5, we show various constraints coming from dark matter physics and inflation in the quartic self-coupling with $\lambda_\chi = \lambda_\phi$ versus the mixing quartic couplings with $\lambda_{\phi\chi} = \lambda_{\chi H}$ in the former and the mixing quartic couplings with $\lambda_{\phi\chi} = \lambda_{\chi H}$ versus the dark matter cubic self-coupling ζ in the latter. Here, we chose the mass parameters near the resonance at $m_{h'} = 3m_\chi$, for instance, $m_\chi = 0.1\,\mathrm{GeV}$ and $m_{h'} = 0.35\,\mathrm{GeV}$. Then, we vary v_ϕ to get the range, $0.209\,\mathrm{GeV} \lesssim m_{Z'} \lesssim 0.418\,\mathrm{GeV}$, depending on λ_ϕ for the fixed g_X and $m_{h'}$. We select four benchmark points in the above plots, $\mathrm{BP}_{\mathrm{SIMP},1}^{\mathrm{mixed}}$, $\mathrm{BP}_{\mathrm{SIMP},1}^{\mathrm{dH}}$, $\mathrm{BP}_{\mathrm{SIMP},2}^{\mathrm{mixed}}$, and $\mathrm{BP}_{\mathrm{SIMP},2}^{\mathrm{dH}}$, with the input parameters summarized in table 2. For the selected benchmark points, we computed inflationary observables, including the spectral index n_s and the tensor-to-scalar ratio r. Note that the scalar power spectrum is normalized to satisfy the latest Planck result.
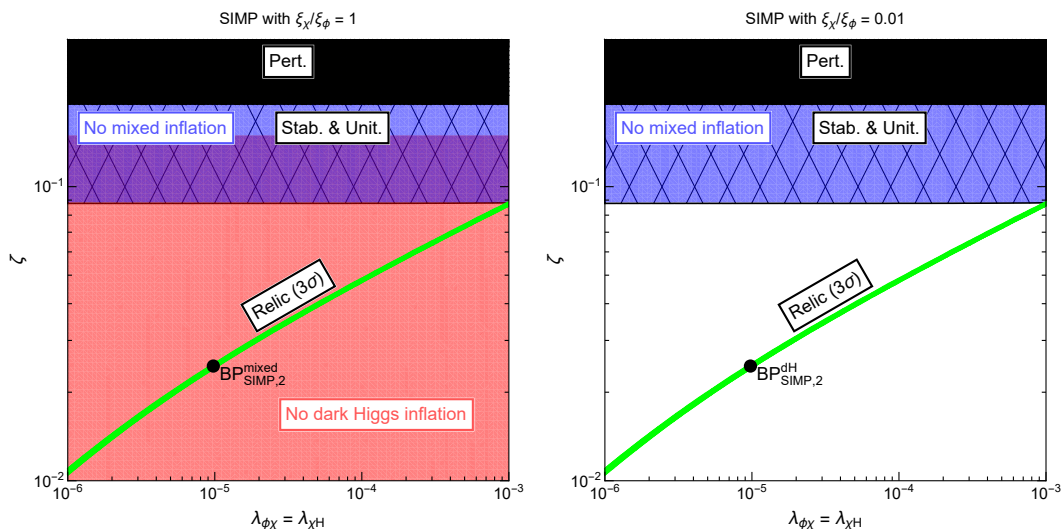
Figure 5. Parameter space for SIMP dark matter scenario with $\xi_\chi/\xi_\phi = 1$ (left) and 0.01 (right), for $\lambda_{\phi\chi} = \lambda_{\chi H}$ versus ζ. The input parameters and color codes are as in figure 4, except that $\lambda_\chi = \lambda_\phi = 0.1$ and ζ is varying.

Benchmark Points	$\lambda_\chi = \lambda_\phi$	$\lambda_{\phi\chi} = \lambda_{\chi H}$	ζ	ξ_χ/ξ_ϕ	n_s	r
$\mathrm{BP}^{\mathrm{mixed}}_{\mathrm{SIMP},1}$	0.1	1.2×10^{-4}	0.05	1	0.9709	0.00337
$\mathrm{BP}^{\mathrm{dH}}_{\mathrm{SIMP},1}$	0.1	1.2×10^{-4}	0.05	0.01	0.9688	0.00292
$\mathrm{BP}^{\mathrm{mixed}}_{\mathrm{SIMP},2}$	0.1	10^{-5}	0.024	1	0.9692	0.00299
$\mathrm{BP}^{\mathrm{dH}}_{\mathrm{SIMP},2}$	0.1	10^{-5}	0.024	0.01	0.9688	0.00292

Table 2. Input parameters for our benchmark points, denoted as black points in figures 4 and 5. In this case, $m_{Z'}$ is also fixed to $m_{Z'} = 0.235\,\mathrm{GeV}$. The superscript represents the inflation type; for example, $\mathrm{BP}^{\mathrm{mixed}}_{\mathrm{SIMP},1}$ ($\mathrm{BP}^{\mathrm{dH}}_{\mathrm{SIMP},1}$) is the benchmark point where mixed (dark Higgs) inflation is allowed.

On the left of figure 6, we show the ζ dependence of the relic density by fixing the other parameters. The relic densities that would have been determined by the WIMP or SIMP channels only are shown in red and green lines on the left of figure 6. The total relic density follows closely the one that would have been determined by SIMP channels only. In comparison, on the right of figure 6, we present the relic density in the plot for the spectral index and the tensor-to-scalar ratio in order to see the correlation between them. We find that the spectral index and the tensor-to-scalar ratio vary, $n_s \approx 0.969$–0.974 and $r \approx 0.0029$–0.0043, depending on the ζ parameter. Thus, the spectral index can deviate sizably from the results of the classical non-minimal coupling inflation, but most of the parameter is still consistent with Planck within about 2σ.
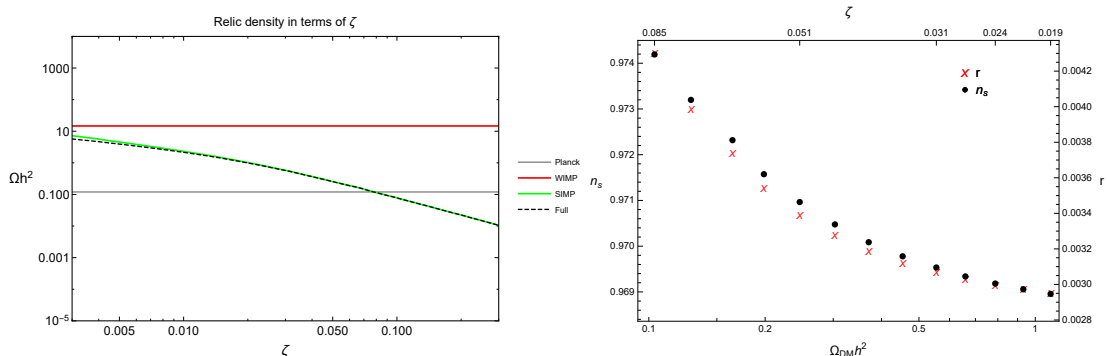
Figure 6. (Left) Relic densities for each dark matter components as a function of ζ. (Right) Correlation between relic density, spectral index and tensor-to-scalar ratio. The parameters are chosen as follows: $\sin\theta = 10^{-6}$, $\varepsilon = 10^{-4}$, $g_X = 0.1$, $m_{h'} = 0.35\,\text{GeV}$, $m_\chi = 0.1\,\text{GeV}$, $\lambda_\phi = \lambda_\chi = 0.1$, $\lambda_{\phi\chi} = \lambda_{\chi H} = 10^{-4}$, thus $m_{Z'} = 0.235\,\text{GeV}$. The grey horizontal solid line on left represents the Planck data for the relic density.

4.4 Forbidden scenarios

For the forbidden dark matter, the hidden sector annihilations are forbidden at zero temperature, but they are open at a finite temperature during the freeze-out [18, 57]. In this case, due to the Boltzmann suppression with $e^{-\Delta\,x}$ for a large dark matter velocity where $\Delta = (m' - m_{\text{DM}})/m_{\text{DM}}$ with m' being the mass of the hidden sector particle, the hidden sector annihilation cross section should be sizable, depending on the mass difference between dark matter and hidden sector particle masses, $m_{h'}$ or $m_{Z'}$, in our case [18]. Importantly, for $T \ll \Delta$, the forbidden annihilation cross section is exponentially suppressed, so the CMB bound on the annihilation cross section for light dark matter does not apply.

For $m_\chi < m_{h'}, m_{Z'}$, we consider the $2 \to 2$ forbidden annihilation processes to be dominant for determining the dark matter relic density. Then, we can approximate the Boltzmann equation (B.1) as

$$
\begin{aligned}
\dot{n}_{\text{DM}} + 3H n_{\text{DM}} &= \langle\sigma v\rangle_{\chi^* h' \to \chi\chi}\left(n_{\text{DM}} n_{h'} - \frac{n_{h'}^{\text{eq}}}{n_{\text{DM}}^{\text{eq}}} n_{\text{DM}}^2\right) + 2\langle\sigma v\rangle_{h'h' \to \chi\chi^*}\left(n_{h'}^2 - \frac{(n_{h'}^{\text{eq}})^2}{(n_{\text{DM}}^{\text{eq}})^2} n_{\text{DM}}^2\right) \\
&\quad + \langle\sigma v\rangle_{\chi^* Z' \to \chi\chi}\left(n_{\text{DM}} n_{Z'} - \frac{n_{Z'}^{\text{eq}}}{n_{\text{DM}}^{\text{eq}}} n_{\text{DM}}^2\right) + 2\langle\sigma v\rangle_{Z'Z' \to \chi\chi^*}\left(n_{Z'}^2 - \frac{(n_{Z'}^{\text{eq}})^2}{(n_{\text{DM}}^{\text{eq}})^2} n_{\text{DM}}^2\right) \\
&\approx -\langle\sigma v\rangle_{\text{FB}}\, n_{\text{DM}}^2\,,
\end{aligned}
\tag{4.15}
$$

with

$$
\begin{aligned}
\langle\sigma v\rangle_{\text{FB}} &\equiv \left(\frac{n_{h'}^{\text{eq}}}{n_{\text{DM}}^{\text{eq}}}\right)\langle\sigma v\rangle_{\chi^* h' \to \chi\chi} + \frac{2(n_{h'}^{\text{eq}})^2}{(n_{\text{DM}}^{\text{eq}})^2}\langle\sigma v\rangle_{h'h' \to \chi\chi^*} \\
&\quad + \left(\frac{n_{Z'}^{\text{eq}}}{n_{\text{DM}}^{\text{eq}}}\right)\langle\sigma v\rangle_{\chi^* Z' \to \chi\chi} + \frac{2(n_{Z'}^{\text{eq}})^2}{(n_{\text{DM}}^{\text{eq}})^2}\langle\sigma v\rangle_{Z'Z' \to \chi\chi^*} \\
&\approx \frac{1}{2}(1+\Delta_{h'})^{3/2} e^{-\Delta_{h'}x}\langle\sigma v\rangle_{\chi^* h' \to \chi\chi} + \frac{1}{2}(1+\Delta_{h'})^3 e^{-2\Delta_{h'}x}\langle\sigma v\rangle_{h'h' \to \chi\chi^*} \\
&\quad + \frac{3}{2}(1+\Delta_{Z'})^{3/2} e^{-\Delta_{Z'}x}\langle\sigma v\rangle_{\chi^* Z' \to \chi\chi} + \frac{9}{2}(1+\Delta_{Z'})^3 e^{-2\Delta_{Z'}x}\langle\sigma v\rangle_{Z'Z' \to \chi\chi^*}\,.
\end{aligned}
\tag{4.16}
$$

Here, the dark matter annihilation rates are computed by using the detailed balance conditions [18, 57]. Then, the general expression for the relic density for forbidden dark matter in our model [18] is given by

$$\Omega_{\rm DM} h^2 = 5.20 \times 10^{-10}\, {\rm GeV}^{-2} \left(\frac{10.75}{g_*}\right)^{1/2} \left(\frac{x_f}{20}\right) \frac{e^{(\Delta_{Z'}+\Delta_{h'})x_f/2} gh}{e^{(\Delta_{Z'}-\Delta_{h'})x_f/2} g + e^{-(\Delta_{Z'}-\Delta_{h'})x_f/2} h}, \tag{4.17}$$

where $\Delta_{h'} = (m_{h'} - m_\chi)/m_\chi$, $\Delta_{Z'} = (m_{Z'} - m_\chi)/m_\chi$, and

$$h(\Delta_{h'}, x_f) \equiv \left[\frac{1}{2} c_1 (1+\Delta_{h'})^{3/2} \left(1 - \Delta_{h'} x_f\, e^{\Delta_{h'} x_f} \int_{\Delta_{h_1} x_f}^\infty dt\, t^{-1} e^{-t}\right)\right.$$
$$\left. + \frac{1}{2} c_2 (1+\Delta_{h'})^3 e^{-\Delta_{h'} x_f} \left(1 - 2\Delta_{h'} x_f\, e^{2\Delta_{h'} x_f} \int_{2\Delta_{h'} x_f}^\infty dt\, t^{-1} e^{-t}\right)\right]^{-1}, \tag{4.18}$$

$$g(\Delta_{Z'}, x_f) \equiv \left[\frac{9 d_1}{2 x_f} (1+\Delta_{Z'})^{3/2} \left(1 - (\Delta_{Z'} x_f)^2 e^{\Delta_{Z'} x_f} \int_{\Delta_{Z'} x_f}^\infty dt\, t^{-2} e^{-t}\right)\right.$$
$$\left. + \frac{9 d_2}{2} (1+\Delta_{Z'})^3 e^{-\Delta_{Z'} x_f} \left(1 - 2(\Delta_{Z'} x_f) e^{2\Delta_{Z'} x_f} \int_{2\Delta_{Z'} x_f}^\infty dt\, t^{-1} e^{-t}\right)\right]^{-1}, \tag{4.19}$$

with $\langle\sigma v\rangle_{h'\chi^* \to \chi\chi} = c_1$, and $\langle\sigma v\rangle_{h'h' \to \chi\chi^*} = c_2$, $\langle\sigma v\rangle_{Z'\chi^* \to \chi\chi} = 6 d_1/x$, and $\langle\sigma v\rangle_{Z'Z' \to \chi\chi^*} = d_2$.

For $m_{h'} \gtrsim m_\chi$ and $m_{Z'} \gg m_{h'}$, the annihilation cross section for the $2 \to 2$ forbidden channels is dominated by the one for $\chi\chi \to \chi^* h'$, approximated to

$$\langle\sigma v\rangle_{\rm FB} \approx \frac{9\zeta^2}{256\pi m_\chi^2} \frac{\sqrt{\Delta_{h'}(1+\Delta_{h'})(4+\Delta_{h'})}}{(2+\Delta_{h'})(3+\Delta_{h'})^2} \left(2(3+\Delta_{h'}) - (1+\Delta_{h'})(5+2\Delta_{h'})\frac{\lambda_{\phi\chi}}{\lambda_\phi}\right)^2 e^{-\Delta_{h'} x}$$
$$\approx \frac{\zeta^2 \sqrt{\Delta_{h'}}}{256\pi m_\chi^2} \left(6 - \frac{5\lambda_{\phi\chi}}{\lambda_\phi}\right)^2 e^{-\Delta_{h'} x}. \tag{4.20}$$

Therefore, the resulting effective annihilation rate depends on the dark matter cubic coupling ζ as well as the mass difference $\Delta_{h'}$ between the resonance and dark matter masses.

In figure 7, we show various constraints coming from dark matter physics and inflation in the quartic self-coupling with $\lambda_\chi = \lambda_\phi$ versus the quartic mixing quartic couplings with $\lambda_{\phi\chi} = \lambda_{\chi H}$ in the former and the quartic mixing quartic couplings with $\lambda_{\phi\chi} = \lambda_{\chi H}$ versus the dark matter cubic self-coupling ζ in the latter. Here, we chose $\Delta_{h'} = (m_{h'} - m_\chi)/m_\chi = 0.4$, for instance, $m_\chi = 0.1\,{\rm GeV}$ and $m_{h'} = 0.16\,{\rm GeV}$, and let v_ϕ vary to get the range, $0.107\,{\rm GeV} \lesssim m_{Z'} \lesssim 0.339\,{\rm GeV}$, depending on λ_ϕ for the fixed g_X and $m_{h'}$. We again selected four benchmark points, $\text{BP}_{\text{FBDM},1}^{\text{mixed}}$, $\text{BP}_{\text{FBDM},1}^{\text{dH}}$, $\text{BP}_{\text{FBDM},2}^{\text{mixed}}$, and $\text{BP}_{\text{FBDM},2}^{\text{dH}}$, with the input parameters shown in table 3. For the selected benchmark points, we computed inflationary observables, including the spectral index n_s and the tensor-to-scalar ratio r.

In order to see the ζ parameter dependence of the relic density and the inflationary predictions. The relic densities corresponding to the WIMP, SIMP and forbidden components are shown in red, green and blue lines on the left of figure 9. The total relic density follows closely the one obtained for forbidden dark matter. In comparison, on the right of
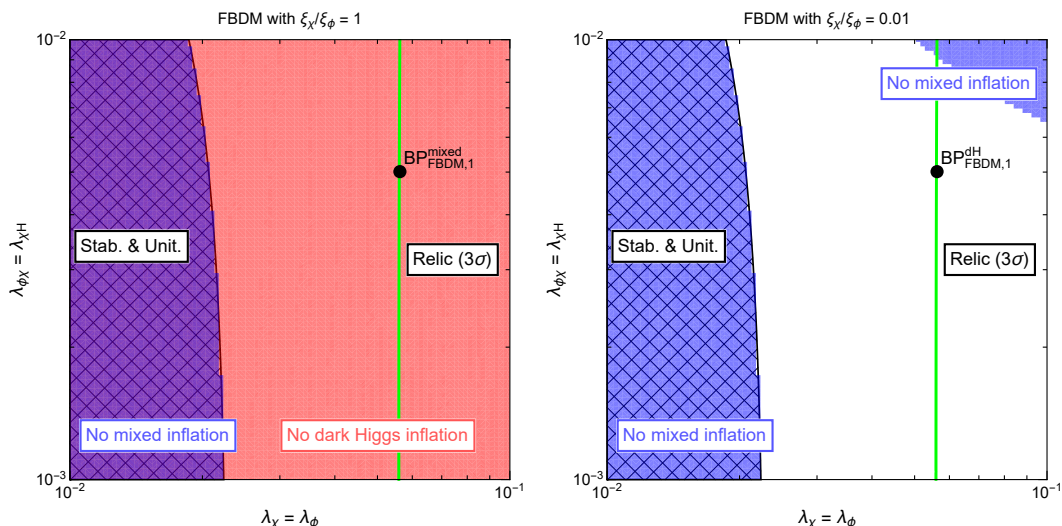
Figure 7. Parameter space for forbidden dark matter scenario with $\xi_\chi/\xi_\phi = 1$ (left) and 0.01 (right) in $\lambda_\chi = \lambda_\phi$ versus $\lambda_{\phi\chi} = \lambda_{\chi H}$. The parameters shown here are set at low-energy scale. The rest input parameters are chosen as $g_X = 0.1$, $\sin\theta = 10^{-5}$, $\varepsilon = 10^{-4}$, $m_{h'} = 0.16\,\text{GeV}$, $m_\chi = 0.1\,\text{GeV}$, and $\zeta = 0.02$. The hatched regions are disfavored due to the stability and unitarity. The dark Higgs (mixed) inflation is not allowed in the red-colored (blue-colored) region. The green solid lines represent the correct dark matter relic abundance within 3σ range [2]. The black points are our benchmark points shown in table 3.

Benchmark Points	$\lambda_\chi = \lambda_\phi$	$\lambda_{\phi\chi} = \lambda_{\chi H}$	ζ	ξ_χ/ξ_ϕ	n_s	r
$\text{BP}^{\text{mixed}}_{\text{FBDM},1}$	0.056	0.005	0.02	1	0.9700	0.00316
$\text{BP}^{\text{dH}}_{\text{FBDM},1}$	0.056	0.005	0.02	0.01	0.9698	0.00312
$\text{BP}^{\text{mixed}}_{\text{FBDM},2}$	0.055	0.002	0.022	1	0.9703	0.00322
$\text{BP}^{\text{dH}}_{\text{FBDM},2}$	0.055	0.002	0.022	0.01	0.9699	0.00313

Table 3. Input parameters for the benchmark points. They correspond to the black points in figures 7 and 8. We chose $g_X = 0.1$, $\sin\theta = 10^{-5}$, $\varepsilon = 10^{-4}$, $m_{h'} = 0.16\,\text{GeV}$ and $m_\chi = 0.1\,\text{GeV}$. The superscript represents the inflation type; for example, $\text{BP}^{\text{mixed}}_{\text{FBDM},1}$ ($\text{BP}^{\text{dH}}_{\text{FBDM},1}$) is the benchmark point where the mixed (dark Higgs) inflation is allowed, etc.

figure 9, we presented the relic density in the plot for the spectral index and the tensor-to-scalar ratio in order to see the correlation between them. We find that the spectral index and the tensor-to-scalar ratio vary, $n_s \approx 0.969$–0.974 and $r \approx 0.0030$–0.0044, depending on the ζ parameter, similarly as in the WIMP and SIMP cases. Thus, the spectral index again can deviate sizably from the results of the classical non-minimal coupling inflation, but most of the parameter is still consistent with Planck within about 2σ.
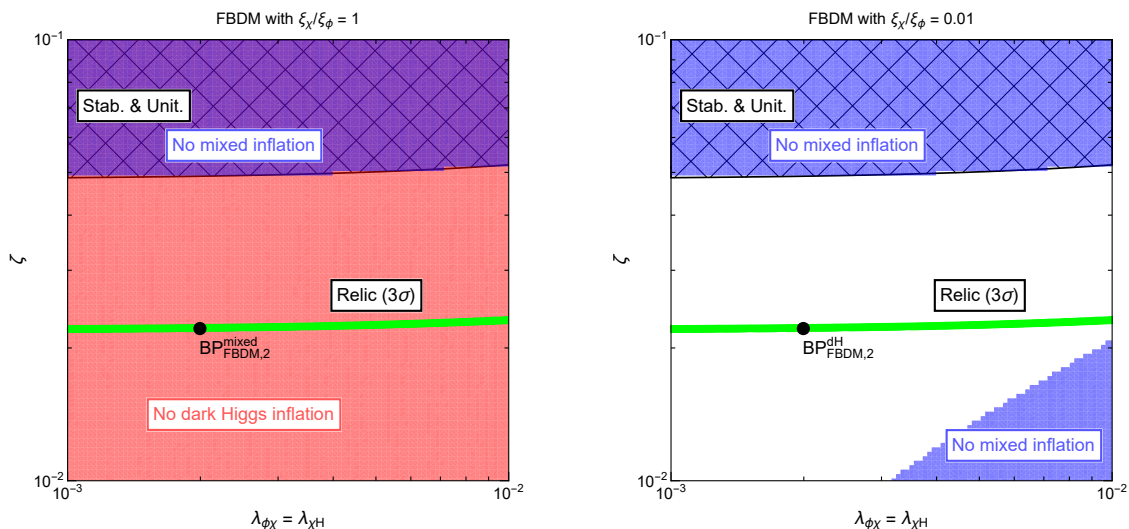
Figure 8. Parameter space for forbidden dark matter scenario with $\xi_\chi/\xi_\phi = 1$ (left) and 0.01 (right) for $\lambda_{\phi\chi} = \lambda_{\chi H}$ versus ζ. The parameters shown here are set at dark matter scale. The rest input parameters and color codes are as in figure 7, except that $\lambda_\chi = \lambda_\phi = 0.055$ and ζ is varying.
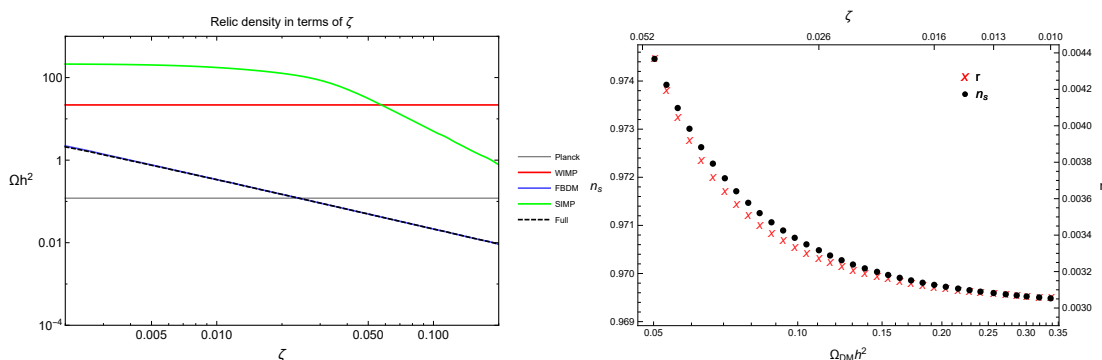

Figure 9. (Left) Relic densities for each dark matter components. (Right) Relic density in the plane of spectral index and tensor-to-scalar ratio. The parameters are chosen as follows: $\sin\theta = 10^{-5}$, $\varepsilon = 10^{-4}$, $g_X = 0.1$, $m_{h'} = 0.16\,\text{GeV}$, $m_\chi = 0.1\,\text{GeV}$, $\lambda_\phi = \lambda_\chi = 0.055$, $\lambda_{\phi\chi} = \lambda_{\chi H} = 0.006$, thus $m_{Z'} = 0.14\,\text{GeV}$. The grey horizontal solid line on left represents the Planck data for the relic density.

5 Conclusions

We have considered the minimal possibility that a complex scalar field beyond Z_2 parity can play roles of both the inflaton and dark matter at the same time. The discussion is focussed upon the models with gauged Z_3 symmetry, which is the remnant of a dark local U(1) symmetry after the spontaneous breakdown. Thus, in this model, dark matter is communicated to the SM through double portals with the Higgs and Z' bosons.

The dark matter cubic self-interaction restricts the inflation with non-minimal couplings to be realized always as either the dark Higgs or the mixture of the dark Higgs and scalar dark matter, but not the pure dark matter direction. Moreover, the same dark

matter cubic self-interaction opens additional channels for dark matter in the dark sector, such as allowed or forbidden $2 \to 2$ (semi-)annihilations and the $3 \to 2$ annihilations, thus it also plays an important role in determining the relic density while evading the stringent constraints from direct and indirect detection experiments.

As a result, we searched for the parameter space for achieving the successful inflation well within the Planck 2σ band as well as the observably consistent dark matter with correct relic abundance, depending on the dominant production mechanism for dark matter. The parameter space in each case of dark matter productions is selected due to the theoretical and phenomenological bounds available from inflation all the way to dark matter energy scales.

A   Renormalization group equations

It is essential to consider renormalization group equations of the relevant parameters to properly connect inflation scale with low-energy scale of dark matter physics. Following refs. [58, 59] (see also refs. [60–62]) and ref. [63], we obtain the renormalization group equations of the model as follows. First, the beta functions for the gauge couplings are

$$(4\pi)^2 \beta_{g_3} = -7 g_3^3 \,, \tag{A.1}$$

$$(4\pi)^2 \beta_g = -\frac{19}{6} g^3 \,, \tag{A.2}$$

$$(4\pi)^2 \beta_{g'} = \frac{41}{6} g'^3 \,, \tag{A.3}$$

$$(4\pi)^2 \beta_{g_X} = \frac{9 s_\phi + s_\chi}{3} g_X^3 \,. \tag{A.4}$$

The beta function for top Yukawa coupling is

$$(4\pi)^2 \beta_{y_t} = y_t \left[\frac{27}{6} y_t^2 - \left(8 g_3^2 + \frac{9}{4} g^2 + \frac{17}{12} g'^2 \right) \right] \,, \tag{A.5}$$

and the beta functions for quartic couplings are

$$(4\pi)^2\beta_{\lambda_H} = 24\lambda_H^2 - 6y_t^4 - 3\lambda_H\left(g'^2 + 3g^2 - 4y_t^2\right) + \frac{3}{8}\left[\left(g'^2 + g^2\right)^2 + 2g^4\right]$$

$$+ \frac{1+s_\chi^2}{2}\lambda_{\chi H}^2 + \frac{1+s_\phi^2}{2}\lambda_{\phi H}^2\,, \tag{A.6}$$

$$(4\pi)^2\beta_{\lambda_{\phi H}} = 6\lambda_{\phi H}\left(2\lambda_H + y_t^2\right) - \frac{3}{2}\lambda_{\phi H}\left(g'^2 + 3g^2 + 36g_X^2\right) + 4s_\phi\lambda_{\phi H}^2$$

$$+ (1+s_\chi^2)\lambda_{\chi H}\lambda_{\phi\chi} + 2(1+3s_\phi^2)\lambda_\phi\lambda_{\phi H}\,, \tag{A.7}$$

$$(4\pi)^2\beta_{\lambda_{\chi H}} = 6\lambda_{\chi H}\left(2\lambda_H + y_t^2\right) - \frac{3}{2}\lambda_{\chi H}\left(g'^2 + 3g^2 + 4g_X^2\right) + 4s_\chi\lambda_{\chi H}^2$$

$$+ (1+s_\phi^2)\lambda_{\phi\chi}\lambda_{\phi H} + 2(1+3s_\chi^2)\lambda_\chi\lambda_{\chi H}\,, \tag{A.8}$$

$$(4\pi)^2\beta_{\lambda_\phi} = 2\lambda_{\phi H}^2 - 108\lambda_\phi g_X^2 + 486g_X^4 + 2\left(1+9s_\phi^2\right)\lambda_\phi^2 + \frac{1+s_\chi^2}{2}\lambda_{\phi\chi}^2\,, \tag{A.9}$$

$$(4\pi)^2\beta_{\lambda_\chi} = 2\lambda_{\chi H}^2 - 12\lambda_\chi g_X^2 + 6g_X^4 + 2\left(1+9s_\chi^2\right)\lambda_\chi^2 + \frac{1+s_\phi^2}{2}\lambda_{\phi\chi}^2 + 9\left(1+s_\phi s_\chi\right)\zeta^2\,, \tag{A.10}$$

$$(4\pi)^2\beta_{\lambda_{\phi\chi}} = 4\lambda_{\chi H}\lambda_{\phi H} - 60\lambda_{\phi\chi}g_X^2 + 108g_X^4 + 2(1+3s_\phi^2)\lambda_\phi\lambda_{\phi\chi} + 2(1+3s_\chi^2)\lambda_\chi\lambda_{\phi\chi}$$

$$+ 4s_\phi s_\chi\lambda_{\phi\chi}^2 + 18(1+s_\chi^2)\zeta^2\,, \tag{A.11}$$

$$(4\pi)^2\beta_\zeta = 6\left(-1+3s_\chi^2\right)\lambda_\chi\zeta + 6s_\phi s_\chi\lambda_{\phi\chi}\zeta - 36g_X^2\zeta\,. \tag{A.12}$$

The beta functions for non-minimal couplings are

$$(4\pi)^2\beta_{\xi_H} = \left(12\lambda_H + 6y_t^2 - \frac{3}{2}g'^2 - \frac{9}{2}g^2\right)\left(\xi_H + \frac{1}{6}\right) + (1+s_\phi)\lambda_{\phi H}\left(\xi_\phi + \frac{1}{6}\right)$$

$$+ (1+s_\chi)\lambda_{\chi H}\left(\xi_\chi + \frac{1}{6}\right)\,, \tag{A.13}$$

$$(4\pi)^2\beta_{\xi_\phi} = 4\lambda_{\phi H}\left(\xi_H + \frac{1}{6}\right) + 2\left[(1+3s_\phi)\lambda_\phi - 27g_X^2\right]\left(\xi_\phi + \frac{1}{6}\right)$$

$$+ (1+s_\chi)\lambda_{\phi\chi}\left(\xi_\chi + \frac{1}{6}\right)\,, \tag{A.14}$$

$$(4\pi)^2\beta_{\xi_\chi} = 4\lambda_{\chi H}\left(\xi_H + \frac{1}{6}\right) + (1+s_\phi)\lambda_{\phi\chi}\left(\xi_\phi + \frac{1}{6}\right)$$

$$+ 2\left[(1+3s_\chi)\lambda_\chi - 3g_X^2\right]\left(\xi_\chi + \frac{1}{6}\right)\,. \tag{A.15}$$

The beta functions for mass parameters are given by

$$(4\pi)^2\beta_{m_H^2} = \left(12\lambda_H + 6y_t^2 - \frac{3g'^2}{2} - \frac{9g^2}{2}\right)m_H^2 + (1+s_\phi)\lambda_{\phi H}m_\phi^2$$

$$- (1+s_\chi)\lambda_{\chi H}m_\chi^2\,, \tag{A.16}$$

$$(4\pi)^2\beta_{m_\phi^2} = 2\left[(1+3s_\phi)\lambda_\phi - 27g_X^2\right]m_\phi^2 + 4\lambda_{\phi H}m_H^2 - (1+s_\chi)\lambda_{\phi\chi}m_\chi^2\,, \tag{A.17}$$

$$(4\pi)^2\beta_{m_\chi^2} = 2\left[(1+3s_\chi)\lambda_\chi - 3g_X^2\right]m_\chi^2 - 4\lambda_{\chi H}m_H^2 - (1+s_\phi)\lambda_{\phi\chi}m_\phi^2\,. \tag{A.18}$$

Finally the anomalous dimensions are given by

$$(4\pi)^2\gamma_H = -\frac{3}{4}g'^2 - \frac{9}{4}g^2 + 3y_t^2\,, \tag{A.19}$$

$$(4\pi)^2\gamma_\phi = -27g_X^2\,, \tag{A.20}$$

$$(4\pi)^2\gamma_\chi = -3g_X^2\,. \tag{A.21}$$

Here, $\beta_p \equiv dp/dt$ for a parameter p and $t = \ln\mu/\mu_0$ with μ being the renormalization scale, $\mu_0 = M_Z$, and s_χ and s_ϕ are the suppression factors that need to be taken into account when inflation occurs along the χ and/or ϕ field direction, or equivalently ψ and φ direction, respectively. They are due to the fact that the presence of the non-minimal couplings modifies the propagators [64, 65]. Explicitly, they are given by

$$s_\phi = \frac{1 + \xi_\phi\varphi^2/M_{\rm P}^2}{1 + (6\xi_\phi + 1)\xi_\phi\varphi^2/M_{\rm P}^2}\,, \tag{A.22}$$

and similarly for s_χ. Note that $s_{\phi,\chi} \to 1$ for $\xi_{\phi,\chi} \to 0$.

B Dark matter annihilation/scattering cross sections

We list the full Boltzmann equation for dark matter relic density and the necessary formulas for the dark matter annihilation and the dark matter-SM scattering as well as the dark matter self-scattering.

Boltzmann equation. The full Boltzmann equation governing the dark matter density, $n_{\rm DM} = n_\chi + n_{\chi*}$, is given [18] by

$$
\begin{aligned}
\dot{n}_{\rm DM} + 3Hn_{\rm DM} = & -\frac{1}{2}\langle\sigma v\rangle_{\chi\chi^*\to f\bar{f}}\left(n_{\rm DM}^2 - (n_{\rm DM}^{\rm eq})^2\right) \\
& -\frac{1}{4}\left(\langle\sigma v^2\rangle_{\chi\chi\chi\to\chi\chi^*} + \langle\sigma v^2\rangle_{\chi\chi\chi^*\to\chi^*\chi^*}\right)\left(n_{\rm DM}^3 - n_{\rm DM}^{\rm eq}n_{\rm DM}^2\right) \\
& -\frac{1}{2}\langle\sigma v^2\rangle_{\chi\chi\chi^*\to\chi h'}\left(n_{\rm DM}^3 - \frac{(n_{\rm DM}^{\rm eq})^2}{n_{h'}^{\rm eq}}n_{\rm DM}n_{h'}\right) \\
& +\langle\sigma v\rangle_{\chi^* h'\to\chi\chi}\left(n_{\rm DM}n_{h'} - \frac{n_{h'}^{\rm eq}}{n_{\rm DM}^{\rm eq}}n_{\rm DM}^2\right) \\
& +2\langle\sigma v\rangle_{h'h'\to\chi\chi^*}\left(n_{h'}^2 - \frac{(n_{h'}^{\rm eq})^2}{(n_{\rm DM}^{\rm eq})^2}n_{\rm DM}^2\right) \\
& -\frac{1}{2}\langle\sigma v^2\rangle_{\chi\chi\chi^*\to\chi Z'}\left(n_{\rm DM}^3 - \frac{(n_{\rm DM}^{\rm eq})^2}{n_{Z'}^{\rm eq}}n_{\rm DM}n_{Z'}\right) \\
& +\langle\sigma v\rangle_{\chi^* Z'\to\chi\chi}\left(n_{\rm DM}n_{Z'} - \frac{n_{Z'}^{\rm eq}}{n_{\rm DM}^{\rm eq}}n_{\rm DM}^2\right) \\
& +2\langle\sigma v\rangle_{Z'Z'\to\chi\chi^*}\left(n_{Z'}^2 - \frac{(n_{Z'}^{\rm eq})^2}{(n_{\rm DM}^{\rm eq})^2}n_{\rm DM}^2\right).
\end{aligned}
\tag{B.1}
$$

Here, we assumed that $n_\chi = n_{\chi^*}$ with no CP violation in the dark sector.

2 → 2 processes. The annihilation cross section of dark matter into a pair of SM fermions [17, 18] is given by

$$\langle\sigma v\rangle_{\chi\chi^*\to\bar{f}f} = \frac{\varepsilon^2 e^2 g_X^2 N_c}{\pi x} \frac{m_\chi^2 + \frac{1}{2}m_f^2}{(4m_\chi^2 - m_{Z'}^2)^2 + m_{Z'}^2\Gamma_{Z'}^2}\sqrt{1 - \frac{m_f^2}{m_\chi^2}}$$
$$+ \frac{N_c}{4\pi}\left(\frac{m_f}{v_{\text{ew}}}\right)^2\left(1 - \frac{m_f^2}{m_\chi^2}\right)^{3/2}\left|\frac{y_{h_1\chi^*\chi}}{4m_\chi^2 - m_{h_1}^2} + \frac{y_{h_2\chi^*\chi}}{4m_\chi^2 - m_{h_2}^2}\right|^2, \quad \text{(B.2)}$$

with $x \equiv m_\chi/T$, $v_{\text{ew}} = 246\,\text{GeV}$, $\varepsilon \simeq \cos\theta_W\xi$ for $\xi \ll 1$ and

$$y_{h_1\chi^*\chi} = -\sin\theta(\lambda_{\phi\chi}v_\phi\cos\theta - \lambda_{\chi H}v\sin\theta), \quad \text{(B.3)}$$
$$y_{h_2\chi^*\chi} = \cos\theta(\lambda_{\phi\chi}v_\phi\sin\theta + \lambda_{\chi H}v\cos\theta), \quad \text{(B.4)}$$

where $h_{1,2}$ are dark Higgs-like and SM Higgs-like scalars [17, 18], respectively, and the mixing angle is given by

$$\tan(2\theta) = \frac{\lambda_{\phi H}v_\phi v_{\text{ew}}}{\lambda_H v_{\text{ew}}^2 - \lambda_\phi v_\phi^2}. \quad \text{(B.5)}$$

The cross section for dark matter annihilating into VV with $V = Z, W$ are given by

$$\langle\sigma v\rangle_{\chi\chi^*\to VV} = \frac{\delta_V e^4}{256\pi\sin^4\theta_W\cos^4\theta_W}\frac{v_{\text{ew}}^2 m_\chi^2}{m_V^4}\left(4 - 4\frac{m_V^2}{m_\chi^2} + 3\frac{m_V^4}{m_\chi^4}\right)$$
$$\times \sqrt{1 - \frac{m_V^2}{m_\chi^2}}\left(\frac{y_{h_1\chi^*\chi}}{4m_\chi^2 - m_{h_1}^2} + \frac{y_{h_2\chi^*\chi}}{4m_\chi^2 - m_{h_2}^2}\right)^2, \quad \text{(B.6)}$$

with $\delta_V = 1$ ($2\cos^4\theta_W$) for $V = Z$ (W). The cross-section for dark matter annihilating into $\gamma\gamma$ is loop-induced, given by

$$\langle\sigma v\rangle_{\chi\chi^*\to\gamma\gamma} = \frac{e^4 m_\chi^2}{64\pi^5 v_{\text{ew}}^2}\left|\sum_f N_c Q_f^2 A_{1/2}(x_f) + A_1(x_w)\right|^2\left(\frac{y_{h_1\chi^*\chi}}{4m_\chi^2 - m_{h_1}^2} + \frac{y_{h_2\chi^*\chi}}{4m_\chi^2 - m_{h_2}^2}\right)^2. \quad \text{(B.7)}$$

The (semi-)annihilation cross sections for the allowed channels for $m_\chi > m_A$ with $A = h', Z'$ are

$$\langle\sigma v\rangle_{\chi\chi\to\chi^*h'} = \frac{3R^2}{128\pi m_\chi^2}\left(1 - \frac{m_{h'}^2}{9m_\chi^2}\right)^{1/2}\left(1 - \frac{m_{h'}^2}{m_\chi^2}\right)^{1/2}\left(\frac{3m_\chi}{v_\phi} - \frac{\lambda_{\phi\chi}v_\phi(9m_\chi^2 + m_{h'}^2)}{m_\chi(3m_\chi^2 - m_{h'}^2)}\right)^2, \quad \text{(B.8)}$$

$$\langle\sigma v\rangle_{\chi\chi^*\to h'h'} = \frac{\lambda_{\phi\chi}^2}{64\pi m_\chi^2}\sqrt{1 - \frac{m_{h'}^2}{m_\chi^2}}\left(1 - \frac{2\lambda_{\phi\chi}v_\phi^2}{2m_\chi^2 - m_{h'}^2} + \frac{6\lambda_\phi v_\phi^2}{4m_\chi^2 - m_{h'}^2}\right)^2, \quad \text{(B.9)}$$

with $R \equiv \zeta v_\phi/m_\chi$ and $m_{h'} \simeq m_{h_1}$, and

$$\langle\sigma v\rangle_{\chi\chi\to\chi^*Z'} = \frac{243 g_X^2 R^2}{64\pi m_{Z'}^2}\left(1 - \frac{m_{Z'}^2}{m_\chi^2}\right)^{3/2}\left(1 - \frac{m_{Z'}^2}{3m_\chi^2}\right)^{-2}\left(1 - \frac{m_{Z'}^2}{9m_\chi^2}\right)^{7/2}, \quad \text{(B.10)}$$

$$\langle\sigma v\rangle_{\chi\chi^*\to Z'Z'} = \frac{g_X^4}{16\pi m_\chi^2}\sqrt{1 - \frac{m_{Z'}^2}{m_\chi^2}}\left(\frac{8m_\chi^4 - 8m_\chi^2 m_{Z'}^2 + 3m_{Z'}^4}{(2m_\chi^2 - m_{Z'}^2)^2} + \frac{54\lambda_{\phi\chi}v_\phi^2}{4m_\chi^2 - m_{h'}^2}\right.$$
$$\left. + \frac{81\lambda_{\phi\chi}^2 v_\phi^4(4m_\chi^4 - 4m_\chi^2 m_{Z'}^2 + 3m_{Z'}^4)}{m_{Z'}^4(4m_\chi^2 - m_{h'}^2)^2}\right). \quad \text{(B.11)}$$

The (semi-)annihilation cross sections for forbidden channels for $m_\chi < m_A$ with $A = h', Z'$ [18] are

$$\langle\sigma v\rangle_{\chi\chi\to\chi^* A} = \frac{n_A}{n_\chi}\langle\sigma v\rangle_{\chi^* A\to\chi\chi},\qquad\text{(B.12)}$$

with

$$\langle\sigma v\rangle_{\chi^* h'\to\chi\chi} = \frac{9R^2}{32\pi m_\chi(m_\chi + m_{h'})}\left(1 - \frac{m_\chi}{m_{h'}}\right)^{1/2}\left(1 + \frac{3m_\chi}{m_{h'}}\right)^{1/2}$$
$$\times\left(\frac{m_\chi}{v_\phi} - \frac{\lambda_{\phi\chi}v_\phi(3m_\chi + 2m_{h'})}{m_{h'}(2m_\chi + m_{h'})}\right)^2,\qquad\text{(B.13)}$$

$$\langle\sigma v\rangle_{\chi^* Z'\to\chi\chi} = \frac{3g_X^2 R^2}{4\pi m_\chi m_{Z'}x}\left(1 + \frac{m_\chi}{m_{Z'}}\right)^{-3}\left(1 + 2\frac{m_\chi}{m_{Z'}}\right)^{-2}\left(1 + 3\frac{m_\chi}{m_{Z'}}\right)^{5/2}\left(1 - \frac{m_\chi}{m_{Z'}}\right)^{1/2}$$
$$\times\left(1 - 4\frac{m_\chi^2}{m_{Z'}^2} + 4\frac{m_\chi^3}{m_{Z'}^3} + 11\frac{m_\chi^4}{m_{Z'}^4}\right),\qquad\text{(B.14)}$$

and

$$\langle\sigma v\rangle_{\chi\chi^*\to AA} = \frac{(n_A)^2}{(n_\chi)^2}\langle\sigma v\rangle_{AA\to\chi\chi^*},\qquad\text{(B.15)}$$

with

$$\langle\sigma v\rangle_{h'h'\to\chi\chi^*} = \frac{\lambda_{\phi\chi}^2}{64\pi m_{h'}^2}\sqrt{1 - \frac{m_\chi^2}{m_{h'}^2}}\left(1 + \frac{2v_\phi^2(\lambda_\phi - \lambda_{\phi\chi})}{m_{h'}^2}\right)^2,\qquad\text{(B.16)}$$

$$\langle\sigma v\rangle_{Z'Z'\to\chi\chi^*} = \frac{g_X^4}{144\pi m_{Z'}^2}\sqrt{1 - \frac{m_\chi^2}{m_{Z'}^2}}\left(11 - \frac{24m_\chi^2}{m_{Z'}^2} + \frac{16m_\chi^4}{m_{Z'}^4}\right.$$
$$\left. - \frac{18\lambda_{\phi\chi}v_\phi^2(4m_\chi^2 - m_{Z'}^2)}{m_{Z'}^2(4m_{Z'}^2 - m_{h'}^2)} + \frac{243\lambda_{\phi\chi}^2 v_\phi^4}{(m_{h'}^2 - 4m_{Z'}^2)^2}\right).\qquad\text{(B.17)}$$

$3 \to 2$ processes. The $3 \to 2$ annihilation cross sections involving only dark matter in the external states[1] are

$$\langle\sigma v^2\rangle_{\chi\chi\chi\to\chi\chi^*} = \frac{\sqrt{5}R^2}{64\pi m_\chi^5}\left(2\lambda_\chi + 9R^2 + \frac{25g_X^2 m_\chi^2}{m_\chi^2 + m_{Z'}^2}\right.$$
$$\left. + \frac{2\lambda_{\phi\chi}m_\chi^2(13m_\chi^2 - 2m_{h'}^2) - \lambda_{\phi\chi}^2 v_\phi^2(19m_\chi^2 - m_{h'}^2)}{(9m_\chi^2 - m_{h'}^2)(m_\chi^2 + m_{h'}^2)}\right)^2,\qquad\text{(B.18)}$$

$$\langle\sigma v^2\rangle_{\chi\chi\chi^*\to\chi^*\chi^*} = \frac{\sqrt{5}R^2}{6144\pi m_\chi^5}\left(74\lambda_\chi - 117R^2 - \frac{200g_X^2 m_\chi^2}{m_\chi^2 + m_{Z'}^2}\right.$$
$$\left. + \frac{24\lambda_{\phi\chi}m_\chi^2(3m_\chi^2 - 2m_{h'}^2) - \lambda_{\phi\chi}^2 v_\phi^2(43m_\chi^2 - 37m_{h'}^2)}{(4m_\chi^2 - m_{h'}^2)(m_\chi^2 + m_{h'}^2)}\right)^2.\qquad\text{(B.19)}$$

---

[1]We have corrected the symmetry factors for initial or final states as compared to refs. [17, 18].

The $3 \to 2$ cross sections with assisted annihilations for $m_\chi > m_A/2$ with $A = h', Z'$ are

$$\langle \sigma v^2 \rangle_{\chi\chi\chi^* \to \chi h'} = \frac{1}{36864\pi m_\chi^5} \left(1 - \frac{m_{h'}^2}{16m_\chi^2}\right)^{1/2} \left(1 - \frac{m_{h'}^2}{4m_\chi^2}\right)^{-3/2}$$

$$\times \left[\frac{192}{7} \frac{m_\chi^2}{v_\phi^2} R^2 \left(1 - \frac{m_{h'}^2}{4m_\chi^2}\right)\left(1 + \frac{m_{h'}^2}{2m_\chi^2}\right)\left(1 - \frac{m_{h'}^2}{7m_\chi^2}\right)^{-1} \right.$$

$$- \frac{192}{7} \lambda_{\phi\chi} R^2 \left(1 - \frac{m_{h'}^2}{7m_\chi^2}\right)^{-1}\left(1 + \frac{25m_{h'}^2}{64m_\chi^2} + \frac{m_{h'}^4}{64m_\chi^4}\right)$$

$$+ 64\lambda_\chi \lambda_{\phi\chi}\left(1 + \frac{m_{h'}^2}{32m_\chi^2}\right) + 16\lambda_{\phi\chi}^2\left(1 - \frac{5m_{h'}^2}{8m_\chi^2}\right)\left(1 + \frac{m_{h'}^2}{2m_\chi^2}\right)^{-1} \quad \text{(B.20)}$$

$$+ 36\lambda_\phi \lambda_{\phi\chi}^2 \frac{v_\phi^2}{m_\chi^2}\left(1 + \frac{m_{h'}^2}{2m_\chi^2}\right)^{-1}$$

$$\left. - 16\lambda_{\phi\chi}^3 \frac{v_\phi^2}{m_\chi^2}\left(1 - \frac{m_{h'}^2}{4m_\chi^2}\right)^{-1}\left(1 + \frac{m_{h'}^2}{2m_\chi^2}\right)^{-1}\left(1 - \frac{23m_{h'}^2}{64m_\chi^2} - \frac{m_{h'}^4}{128m_\chi^4}\right) \right]^2 ,$$

$$\langle \sigma v^2 \rangle_{\chi\chi\chi^* \to \chi Z'} = \frac{g_X^2}{1728\pi m_\chi^5}\frac{m_{Z'}^2}{m_\chi^2}\left(1 - \frac{m_{Z'}^2}{16m_\chi^2}\right)^{3/2}\left(1 - \frac{m_{Z'}^2}{4m_\chi^2}\right)^{-1/2}$$

$$\times \left(2\lambda_\chi - \frac{12g_X^2 m_\chi^2}{2m_\chi^2 + m_{Z'}^2} - \frac{3R^2(192m_\chi^4 - 31m_\chi^2 m_{Z'}^2 + m_{Z'}^4)}{m_{Z'}^2(7m_\chi^2 - m_{Z'}^2)} \right.$$

$$\left. + \frac{16\lambda_{\phi\chi}m_\chi^2(4m_\chi^2 - m_{Z'}^2)}{(4m_\chi^2 - m_{h'}^2)(2m_\chi^2 + m_{Z'}^2)} + \frac{\lambda_{\phi\chi}^2 v_\phi^2}{4m_\chi^2 - m_{h'}^2}\right)^2 . \quad \text{(B.21)}$$

DM-SM scatterings. The effective Lagrangian for dark matter-quark elastic scattering is given by

$$\mathcal{L}_{q,\text{eff}} = \frac{m_q}{v_{\text{ew}}}\left(\frac{y_{h_2\chi^*\chi}}{m_{h_2}^2} + \frac{y_{h_1\chi^*\chi}}{m_{h_1}^2}\right)|\chi|^2\bar{q}q + \frac{g_X q_\chi e \,\varepsilon Q_q}{m_{Z'}^2}\, i(\chi\partial_\mu\chi^* - \chi^*\partial_\mu\chi)\bar{q}\gamma^\mu q . \quad \text{(B.22)}$$

Then, the relevant matching conditions between quark and nucleon operators are given by

$$\langle N|\bar{q}q|N\rangle = \frac{m_N}{m_q} f_{Tq}^{(N)} , \quad \text{(B.23)}$$

for light quarks ($q = u, d, s$), and

$$\langle N|\bar{q}q|N\rangle = \frac{2}{27}\frac{m_N}{m_q} f_{TG}^{(N)} , \quad f_{TG}^{(N)} = 1 - \sum_{q=u,d,s} f_{Tq}^{(N)} , \quad \text{(B.24)}$$

for heavy quarks ($q = c, b, t$), and those for vector operators are given by

$$\begin{aligned}
\langle N|\bar{u}\gamma^\mu u|N\rangle &= 2\bar{N}\gamma^\mu N , \quad N = p , \\
\langle N|\bar{d}\gamma^\mu d|N\rangle &= \bar{N}\gamma^\mu N , \quad\;\; N = p , \\
\langle N|\bar{u}\gamma^\mu u|N\rangle &= \bar{N}\gamma^\mu N , \quad\;\; N = n , \\
\langle N|\bar{d}\gamma^\mu d|N\rangle &= 2\bar{N}\gamma^\mu N , \quad N = n .
\end{aligned} \quad \text{(B.25)}$$

As a result, we get the effective Lagrangian for dark matter-nucleon elastic scattering as follows,

$$\mathcal{L}_{N,\text{eff}} = \frac{m_N}{v_{\text{ew}}}\left(\frac{y_{h_2\chi^*\chi}}{m_{h_2}^2} + \frac{y_{h_1\chi^*\chi}}{m_{h_1}^2}\right)\left(\sum_{q=u,d,s} f_{Tq}^{(N)} + \frac{2}{27}f_{TG}^{(N)} \times 3\right)|\chi|^2\bar{N}N$$
$$+ \frac{g_X q_\chi e\,\varepsilon}{m_{Z'}^2}\,i(\chi\partial_\mu\chi^* - \chi^*\partial_\mu\chi)\Big((2Q_u + Q_d)\bar{p}\gamma^\mu p + (Q_u + 2Q_d)\bar{n}\gamma^\mu n\Big), \quad \text{(B.26)}$$

where $y_{h_1\chi^*\chi}$ and $y_{h_2\chi^*\chi}$ are given in eqs. (B.3) and (B.4), respectively. Thus, from $2Q_u + Q_d = +1$ and $Q_u + 2Q_d = 0$, there is a nonzero interaction only for dark matter-proton scattering with Z' portal. Consequently, we obtained the χ-nucleus scattering cross section as follows,

$$\sigma_{\chi-A} = \frac{\mu_A^2}{4\pi m_\chi^2}\Big[Z\big(c_p f_p + g_p\big) + (A-Z)\big(c_n f_n + g_n\big)\Big]^2, \quad \text{(B.27)}$$

where $\mu_A = m_\chi m_A/(m_A + m_\chi)$ is the reduced mass of the dark matter-nucleus system with m_A being the target nucleus mass, Z, A are the number of protons and the atomic number, respectively, and the effective couplings and form factors [66, 67] are given by

$$c_N \equiv \frac{m_N}{v_{\text{ew}}}\left(\frac{y_{h_2\chi^*\chi}}{m_{h_2}^2} + \frac{y_{h_1\chi^*\chi}}{m_{h_1}^2}\right),$$
$$f_p \equiv \sum_{q=u,d,s} f_{Tq}^{(p)} + \frac{2}{9}f_{TG}^{(p)} \simeq 0.28,$$
$$f_n \equiv \sum_{q=u,d,s} f_{Tq}^{(n)} + \frac{2}{9}f_{TG}^{(n)} \simeq 0.28, \quad \text{(B.28)}$$
$$g_p = -\frac{2eq_\chi g_X\varepsilon m_\chi}{m_{Z'}^2},$$
$$g_n \approx 0.$$

Similarly, the χ^*-nucleus scattering cross section has the Z' contributions flipped in sign, given by

$$\sigma_{\chi^*-A} = \frac{\mu_A^2}{4\pi m_\chi^2}\Big[Z\big(c_p f_p - g_p\big) + (A-Z)\big(c_n f_n - g_n\big)\Big]^2. \quad \text{(B.29)}$$

Then, the averaged dark matter-nucleus scattering cross section is given

$$\sigma_{\text{DM}-A} = \frac{1}{2}\Big(\sigma_{\chi-A} + \sigma_{\chi^*-A}\Big). \quad \text{(B.30)}$$

The above dark matter-nucleus scattering cross section is related to the normalized-to-proton scattering cross section [66, 67], $\sigma_{\text{DM}-p}$, that is usually presented for experimental limits, by

$$\sigma_{\text{DM}-p} = \left(\frac{\mu_N}{\mu_A}\right)^2 \frac{\sigma_{\text{DM}-A}}{A^2}, \quad \text{(B.31)}$$

with $\mu_N = m_\chi m_N/(m_N + m_\chi)$.

The elastic scattering between dark matter and electron is mediated by CP-even scalars and Z', so the corresponding cross section is similarly given by

$$\sigma_{\mathrm{DM}-e} = \frac{\mu_e^2}{8\pi m_\chi^2}\left[\frac{m_e}{v_{\mathrm{ew}}}\left(\frac{y_{h_2\chi^*\chi}}{m_{h_2}^2} + \frac{y_{h_1\chi^*\chi}}{m_{h_1}^2}\right) + \frac{2eq_\chi g_X \varepsilon m_\chi}{m_{Z'}^2}\right]^2$$
$$+ \frac{\mu_e^2}{8\pi m_\chi^2}\left[\frac{m_e}{v_{\mathrm{ew}}}\left(\frac{y_{h_2\chi^*\chi}}{m_{h_2}^2} + \frac{y_{h_1\chi^*\chi}}{m_{h_1}^2}\right) - \frac{2eq_\chi g_X \varepsilon m_\chi}{m_{Z'}^2}\right]^2$$
$$= \frac{\mu_e^2}{4\pi m_\chi^2}\left[\frac{m_e^2}{v_{\mathrm{ew}}^2}\left(\frac{y_{h_2\chi^*\chi}}{m_{h_2}^2} + \frac{y_{h_1\chi^*\chi}}{m_{h_1}^2}\right)^2 + \frac{4e^2 q_\chi^2 g_X^2 \varepsilon^2 m_\chi^2}{m_{Z'}^4}\right], \qquad (\text{B.32})$$

where $\mu_e = m_\chi m_e/(m_e + m_\chi)$ is the reduced mass of the dark matter-electron system.

DM self-scattering. The self-interaction cross section for scalar dark matter in our model is given [17] by

$$\sigma_{\mathrm{self}} = \frac{1}{64\pi m_\chi^2}\left(|\mathcal{M}_{\chi\chi}|^2 + |\mathcal{M}_{\chi\chi^*}|^2\right), \qquad (\text{B.33})$$

where the squared amplitudes are given by

$$|\mathcal{M}_{\chi\chi}|^2 = 2\left(2\lambda_\chi + \frac{3\zeta^2 m_{h'}^2}{\lambda_\phi m_\chi^2} + \frac{8\lambda_\phi m_\chi^2}{9m_{h'}^2} - \frac{\lambda_{\phi\chi}^2}{2\lambda_\phi}\right)^2, \qquad (\text{B.34})$$

$$|\mathcal{M}_{\chi\chi^*}|^2 = 4\left(2\lambda_\chi - \frac{9\zeta^2 m_{h'}^2}{2\lambda_\phi m_\chi^2} - \frac{4\lambda_\phi m_\chi^2}{m_{h'}^2} + \frac{\lambda_{\phi\chi}^2(m_{h'}^2 - 2m_\chi^2)}{2\lambda_\phi(4m_\chi^2 - m_{h'}^2)}\right)^2. \qquad (\text{B.35})$$

References

[1] PLANCK collaboration, *Planck 2018 results. X. Constraints on inflation*, [arXiv:1807.06211](#) [INSPIRE].

[2] PLANCK collaboration, *Planck 2018 results. VI. Cosmological parameters*, [arXiv:1807.06209](#) [INSPIRE].

[3] F.L. Bezrukov and M. Shaposhnikov, *The Standard Model Higgs boson as the inflaton*, [*Phys. Lett. B* **659** (2008) 703](#) [[arXiv:0710.3755](#)] [INSPIRE].

[4] R.N. Lerner and J. McDonald, *Gauge singlet scalar as inflaton and thermal relic dark matter*, [*Phys. Rev. D* **80** (2009) 123507](#) [[arXiv:0909.0520](#)] [INSPIRE].

[5] J.-O. Gong, H.M. Lee and S.K. Kang, *Inflation and dark matter in two Higgs doublet models*, [*JHEP* **04** (2012) 128](#) [[arXiv:1202.0288](#)] [INSPIRE].

[6] N. Haba and R. Takahashi, *Higgs inflation with singlet scalar dark matter and right-handed neutrino in light of BICEP2*, [*Phys. Rev. D* **89** (2014) 115009](#) [*Erratum ibid.* **90** (2014) 039905] [[arXiv:1404.4737](#)] [INSPIRE].

[7] T. Tenkanen, K. Tuominen and V. Vaskonen, *A Strong Electroweak Phase Transition from the Inflaton Field*, *JCAP* **09** (2016) 037 [arXiv:1606.06063] [INSPIRE].

[8] A. Aravind, M. Xiao and J.-H. Yu, *Higgs Portal to Inflation and Fermionic Dark Matter*, *Phys. Rev. D* **93** (2016) 123513 [*Erratum ibid.* **96** (2017) 069901] [arXiv:1512.09126] [INSPIRE].

[9] G. Ballesteros, J. Redondo, A. Ringwald and C. Tamarit, *Standard Model-axion-seesaw-Higgs portal inflation. Five problems of particle physics and cosmology solved in one stroke*, *JCAP* **08** (2017) 001 [arXiv:1610.01639] [INSPIRE].

[10] D. Hooper, G. Krnjaic, A.J. Long and S.D. Mcdermott, *Can the Inflaton Also Be a Weakly Interacting Massive Particle?*, *Phys. Rev. Lett.* **122** (2019) 091802 [arXiv:1807.03308] [INSPIRE].

[11] S.-M. Choi, Y.-J. Kang, H.M. Lee and K. Yamashita, *Unitary inflaton as decaying dark matter*, *JHEP* **05** (2019) 060 [arXiv:1902.03781] [INSPIRE].

[12] J. Kim, P. Ko and W.-I. Park, *Higgs-portal assisted Higgs inflation with a sizeable tensor-to-scalar ratio*, *JCAP* **02** (2017) 003 [arXiv:1405.1635] [INSPIRE].

[13] Y. Hochberg, E. Kuflik, T. Volansky and J.G. Wacker, *Mechanism for Thermal Relic Dark Matter of Strongly Interacting Massive Particles*, *Phys. Rev. Lett.* **113** (2014) 171301 [arXiv:1402.5143] [INSPIRE].

[14] Y. Hochberg, E. Kuflik, H. Murayama, T. Volansky and J.G. Wacker, *Model for Thermal Relic Dark Matter of Strongly Interacting Massive Particles*, *Phys. Rev. Lett.* **115** (2015) 021301 [arXiv:1411.3727] [INSPIRE].

[15] H.M. Lee and M.-S. Seo, *Communication with SIMP dark mesons via Z'-portal*, *Phys. Lett. B* **748** (2015) 316 [arXiv:1504.00745] [INSPIRE].

[16] Y. Hochberg, E. Kuflik, R. Mcgehee, H. Murayama and K. Schutz, *Strongly interacting massive particles through the axion portal*, *Phys. Rev. D* **98** (2018) 115031 [arXiv:1806.10139] [INSPIRE].

[17] S.-M. Choi and H.M. Lee, *SIMP dark matter with gauged Z_3 symmetry*, *JHEP* **09** (2015) 063 [arXiv:1505.00960] [INSPIRE].

[18] S.-M. Choi, Y.-J. Kang and H.M. Lee, *On thermal production of self-interacting dark matter*, *JHEP* **12** (2016) 099 [arXiv:1610.04748] [INSPIRE].

[19] C.P. Burgess, H.M. Lee and M. Trott, *Power-counting and the Validity of the Classical Approximation During Inflation*, *JHEP* **09** (2009) 103 [arXiv:0902.4465] [INSPIRE].

[20] J.L.F. Barbon and J.R. Espinosa, *On the Naturalness of Higgs Inflation*, *Phys. Rev. D* **79** (2009) 081302 [arXiv:0903.0355] [INSPIRE].

[21] C.P. Burgess, H.M. Lee and M. Trott, *Comment on Higgs Inflation and Naturalness*, *JHEP* **07** (2010) 007 [arXiv:1002.2730] [INSPIRE].

[22] M.P. Hertzberg, *On Inflation with Non-minimal Coupling*, *JHEP* **11** (2010) 023 [arXiv:1002.2995] [INSPIRE].

[23] G.F. Giudice and H.M. Lee, *Unitarizing Higgs Inflation*, *Phys. Lett. B* **694** (2011) 294 [arXiv:1010.1417] [INSPIRE].

[24] H.M. Lee, *Running inflation with unitary Higgs*, *Phys. Lett. B* **722** (2013) 198 [arXiv:1301.1787] [INSPIRE].

[25] H.M. Lee, *Light inflaton completing Higgs inflation*, *Phys. Rev. D* **98** (2018) 015020 [arXiv:1802.06174] [INSPIRE].

[26] Y. Ema, *Higgs Scalaron Mixed Inflation*, *Phys. Lett. B* **770** (2017) 403 [arXiv:1701.07665] [INSPIRE].

[27] Y. Ema, K. Mukaida and J. van de Vis, *Higgs Inflation as Nonlinear σ-model and Scalaron as its σ-meson*, arXiv:2002.11739 [INSPIRE].

[28] P. Ko and Y. Tang, *Self-interacting scalar dark matter with local Z_3 symmetry*, *JCAP* **05** (2014) 047 [arXiv:1402.6449] [INSPIRE].

[29] P. Ko and Y. Tang, *Galactic center γ-ray excess in hidden sector DM models with dark gauge symmetries: local Z_3 symmetry as an example*, *JCAP* **01** (2015) 023 [arXiv:1407.5492] [INSPIRE].

[30] S.-M. Choi and H.M. Lee, *Resonant SIMP dark matter*, *Phys. Lett. B* **758** (2016) 47 [arXiv:1601.03566] [INSPIRE].

[31] O. Lebedev and H.M. Lee, *Higgs Portal Inflation*, *Eur. Phys. J. C* **71** (2011) 1821 [arXiv:1105.2284] [INSPIRE].

[32] M. Sher, *Electroweak Higgs Potentials and Vacuum Stability*, *Phys. Rept.* **179** (1989) 273 [INSPIRE].

[33] E.D. Stewart and D.H. Lyth, *A More accurate analytic calculation of the spectrum of cosmological perturbations produced during inflation*, *Phys. Lett. B* **302** (1993) 171 [gr-qc/9302019] [INSPIRE].

[34] A.R. Liddle, P. Parsons and J.D. Barrow, *Formalizing the slow roll approximation in inflation*, *Phys. Rev. D* **50** (1994) 7222 [astro-ph/9408015] [INSPIRE].

[35] S.M. Leach, A.R. Liddle, J. Martin and D.J. Schwarz, *Cosmological parameter estimation and the inflationary cosmology*, *Phys. Rev. D* **66** (2002) 023515 [astro-ph/0202094] [INSPIRE].

[36] S.-M. Choi and H.M. Lee, *Inflection point inflation and reheating*, *Eur. Phys. J. C* **76** (2016) 303 [arXiv:1601.05979] [INSPIRE].

[37] CMS collaboration, *Search for invisible decays of a Higgs boson produced through vector boson fusion in proton-proton collisions at $\sqrt{s} = 13\,TeV$*, *Phys. Lett. B* **793** (2019) 520 [arXiv:1809.05937] [INSPIRE].

[38] R. Essig, T. Volansky and T.-T. Yu, *New Constraints and Prospects for sub-GeV Dark Matter Scattering off Electrons in Xenon*, *Phys. Rev. D* **96** (2017) 043017 [arXiv:1703.00910] [INSPIRE].

[39] XENON collaboration, *First Dark Matter Search Results from the XENON1T Experiment*, *Phys. Rev. Lett.* **119** (2017) 181301 [arXiv:1705.06655] [INSPIRE].

[40] XENON collaboration, *Dark Matter Search Results from a One Ton-Year Exposure of XENON1T*, *Phys. Rev. Lett.* **121** (2018) 111302 [arXiv:1805.12562] [INSPIRE].

[41] M. Battaglieri et al., *US Cosmic Visions: New Ideas in Dark Matter 2017: Community Report*, in *U.S. Cosmic Visions: New Ideas in Dark Matter*, (2017) [arXiv:1707.04591] [INSPIRE].

[42] T.R. Slatyer, *Indirect dark matter signatures in the cosmic dark ages. I. Generalizing the bound on s-wave dark matter annihilation from Planck results*, *Phys. Rev. D* **93** (2016) 023527 [arXiv:1506.03811] [INSPIRE].

[43] A. Cuoco, J. Heisig, M. Korsmeier and M. Krämer, *Constraining heavy dark matter with cosmic-ray antiprotons*, *JCAP* **04** (2018) 004 [arXiv:1711.05274] [INSPIRE].

[44] G. Giesen et al., *AMS-02 antiprotons, at last! Secondary astrophysical component and immediate implications for Dark Matter*, *JCAP* **09** (2015) 023 [arXiv:1504.04276] [INSPIRE].

[45] L. Bergstrom, T. Bringmann, I. Cholis, D. Hooper and C. Weniger, *New Limits on Dark Matter Annihilation from AMS Cosmic Ray Positron Data*, *Phys. Rev. Lett.* **111** (2013) 171101 [arXiv:1306.3983] [INSPIRE].

[46] FERMI-LAT collaboration, *Searching for Dark Matter Annihilation from Milky Way Dwarf Spheroidal Galaxies with Six Years of Fermi Large Area Telescope Data*, *Phys. Rev. Lett.* **115** (2015) 231301 [arXiv:1503.02641] [INSPIRE].

[47] FERMI-LAT collaboration, *Updated search for spectral lines from Galactic dark matter interactions with pass 8 data from the Fermi Large Area Telescope*, *Phys. Rev. D* **91** (2015) 122002 [arXiv:1506.00013] [INSPIRE].

[48] H.E.S.S. collaboration, *Search for dark matter annihilations towards the inner Galactic halo from 10 years of observations with H.E.S.S*, *Phys. Rev. Lett.* **117** (2016) 111301 [arXiv:1607.08142] [INSPIRE].

[49] HESS collaboration, *Dark matter gamma-ray line searches toward the Galactic Center halo with H.E.S.S. I*, *PoS* **ICRC2017** (2018) 893 [arXiv:1708.08358] [INSPIRE].

[50] M. Markevitch et al., *Direct constraints on the dark matter self-interaction cross-section from the merging galaxy cluster 1E0657-56*, *Astrophys. J.* **606** (2004) 819 [astro-ph/0309303] [INSPIRE].

[51] D. Clowe, A. Gonzalez and M. Markevitch, *Weak lensing mass reconstruction of the interacting cluster 1E0657-558: Direct evidence for the existence of dark matter*, *Astrophys. J.* **604** (2004) 596 [astro-ph/0312273] [INSPIRE].

[52] S.W. Randall, M. Markevitch, D. Clowe, A.H. Gonzalez and M. Bradac, *Constraints on the Self-Interaction Cross-Section of Dark Matter from Numerical Simulations of the Merging Galaxy Cluster 1E 0657-56*, *Astrophys. J.* **679** (2008) 1173 [arXiv:0704.0261] [INSPIRE].

[53] A.H.G. Peter, M. Rocha, J.S. Bullock and M. Kaplinghat, *Cosmological Simulations with Self-Interacting Dark Matter II: Halo Shapes vs. Observations*, *Mon. Not. Roy. Astron. Soc.* **430** (2013) 105 [arXiv:1208.3026] [INSPIRE].

[54] S. Tulin and H.-B. Yu, *Dark Matter Self-interactions and Small Scale Structure*, *Phys. Rept.* **730** (2018) 1 [arXiv:1705.02358] [INSPIRE].

[55] S.-M. Choi, H.M. Lee and M.-S. Seo, *Cosmic abundances of SIMP dark matter*, *JHEP* **04** (2017) 154 [arXiv:1702.07860] [INSPIRE].

[56] S.-M. Choi, H.M. Lee, P. Ko and A. Natale, *Resolving phenomenological problems with strongly-interacting-massive-particle models with dark vector resonances*, *Phys. Rev. D* **98** (2018) 015034 [arXiv:1801.07726] [INSPIRE].

[57] R.T. D'Agnolo and J.T. Ruderman, *Light Dark Matter from Forbidden Channels*, *Phys. Rev. Lett.* **115** (2015) 061301 [arXiv:1505.07107] [INSPIRE].

[58] M.-x. Luo, H.-w. Wang and Y. Xiao, *Two loop renormalization group equations in general gauge field theories*, *Phys. Rev. D* **67** (2003) 065019 [hep-ph/0211440] [INSPIRE].

[59] M.-x. Luo and Y. Xiao, *Two loop renormalization group equations in the standard model*, *Phys. Rev. Lett.* **90** (2003) 011601 [`hep-ph/0207271`] [INSPIRE].

[60] M.E. Machacek and M.T. Vaughn, *Two Loop Renormalization Group Equations in a General Quantum Field Theory. 1. Wave Function Renormalization*, *Nucl. Phys. B* **222** (1983) 83 [INSPIRE].

[61] M.E. Machacek and M.T. Vaughn, *Two Loop Renormalization Group Equations in a General Quantum Field Theory. 2. Yukawa Couplings*, *Nucl. Phys. B* **236** (1984) 221 [INSPIRE].

[62] M.E. Machacek and M.T. Vaughn, *Two Loop Renormalization Group Equations in a General Quantum Field Theory. 3. Scalar Quartic Couplings*, *Nucl. Phys. B* **249** (1985) 70 [INSPIRE].

[63] I.L. Buchbinder, S.D. Odintsov and I.L. Shapiro, *Effective action in quantum gravity*, Bristol, U.K., IOP (1992) [INSPIRE].

[64] D.S. Salopek, J.R. Bond and J.M. Bardeen, *Designing Density Fluctuation Spectra in Inflation*, *Phys. Rev. D* **40** (1989) 1753 [INSPIRE].

[65] A. De Simone, M.P. Hertzberg and F. Wilczek, *Running Inflation in the Standard Model*, *Phys. Lett. B* **678** (2009) 1 [`arXiv:0812.4946`] [INSPIRE].

[66] A. Carrillo-Monteverde, Y.-J. Kang, H.M. Lee, M. Park and V. Sanz, *Dark Matter Direct Detection from new interactions in models with spin-two mediators*, *JHEP* **06** (2018) 037 [`arXiv:1803.02144`] [INSPIRE].

[67] Y.-J. Kang and H.M. Lee, *Lightening Gravity-Mediated Dark Matter*, `arXiv:2001.04868` [INSPIRE].